

# Collisional charging of dust particles by suprathermal plasmas.

## II - Regularized Kappa distributions

Rudi Gaelzer<sup>1, a)</sup> and Luiz F. Ziebell<sup>1, b)</sup>

*Instituto de Física, Universidade Federal do Rio Grande do Sul, CP 15051, Porto Alegre, Rio Grande do Sul, 91501-970, Brazil*

(Dated: February 11, 2025)

We study the effects of the velocity distribution functions of the plasma particles on the equilibrium charge of dust grains, acquired through inelastic collisions of the particles with the grains. This paper is the second in a series of two papers on the subject. Here, we consider the charging process when the plasma particles are statistically described by the recently proposed regularized Kappa distribution functions, which allow for extreme suprathermal states, characterized by extremely low values of the kappa index, previously forbidden to the standard Kappa distributions, whose effects on dust charging were studied in Paper I of this series. We analyse the effects that extreme suprathermal states of the plasma particles have on dust charging and verify conditions for the uncommon result of positive equilibrium charge, employing two different models for the regularized Kappa distributions, one with kinetic temperature dependent on the kappa index, and another where the temperature is kappa-independent.

**Keywords:** Dusty plasmas, Regularized Kappa distribution, Kinetic theory of plasmas, Charging of dust grains.

### I. INTRODUCTION

Space and astrophysical plasmas are rarely composed by electrons and ionized atoms alone, but usually contain a variable fraction of their total mass in form of contaminants ranging from nanoparticles to heavier bodies with various chemical compositions and shapes. These contaminants in different plasma environments are usually referred to as “dust”, and can have different origins. In planetary systems, dust can be produced by volcanism, collisions between asteroids, or be present in planetary rings and comet tails. Dust is also present in the interstellar medium and can comprise a significant part of the stellar winds emanating from carbon-rich stars, as inferred from spectroscopic studies in the infrared region. There are several reviews available in the literature discussing the origin and composition of dust in space and laboratory plasmas, of which Refs. 1–12 are a representative sample.

Recently, observations from the James Webb Space Telescope, processed with a new spectroscopic technique, have given direct evidence of carbon-enriched stellar wind emanating in form of dust shells from the orbiting Wolf-Rayet binary WR 140.<sup>13</sup> The dust shells are propagating outward with a measured velocity consistent with the theoretical wind speed and the distance between the shells correlates with the period of maximum dust production by the binary, which is associated with the orbital period of the pair.

The dust contained in a space plasma environment acquires an electric charge through a number of mechanisms, the most important of which are: absorption

of plasma particles due to inelastic collisions, photoionization, secondary electron emission and field emission. Refs. 4, 6, 8, 11, 12, 14–19, among others, give detailed account on the most important charging mechanisms for space plasmas. After acquiring electric charge, the dust grains start to interact with the plasma particles not only through collisions, but also via electromagnetic fields. This complex system is then referred to as “dusty plasma”.

Although the dust grains in space and astrophysical plasmas are almost always subjected to more than one of the charging processes mentioned above, each with varying degree of importance on the final charge due to circumstances such as density and temperature of the plasma, magnetic field, ultraviolet flux intensity and chemical composition, a detailed description of each process is a complex task that demands expertise not only on plasma physics, but also on quantum physics and materials research. Moreover, the final result can mask the detailed processes that take place in a particular charging mechanism. Therefore, in the present series of two papers we investigate solely the collisional charging of dust grains immersed in Kappa plasmas, in order to stress the particular physics involved in this process.

One important effect due to the presence of dust in a plasma is related to the propagation of electrostatic or electromagnetic waves and their interaction with the plasma particles and dust grains. The presence of dust gives rise to entirely new wave modes, which are of extremely low frequency, on the order of the dust plasma or dust cyclotron frequencies.<sup>4,20–24</sup> Moreover, the dust component also affects the usual wave modes propagating in the plasma, particularly the Alfvén waves.<sup>25–37</sup>

On the other hand, space plasma environments are usually found in a turbulent (quasi-) steady state that is far from the thermodynamic equilibrium.<sup>38–42</sup> Of par-

<sup>a)</sup> Electronic mail: [rudi.gaelzer@ufrgs.br](mailto:rudi.gaelzer@ufrgs.br)

<sup>b)</sup> Electronic mail: [luiz.ziebell@ufrgs.br](mailto:luiz.ziebell@ufrgs.br)

ticular importance for the kinetic theory of space plasmas are the velocity distribution functions (VDFs) that better describe the statistical distribution of velocities of the plasma particles. In recent years, it has become a consensus in the space plasma community that the VDFs that describe the turbulent state of the plasma have distinct nonthermal features, such as high-energy tails that follow a power-law dependency, instead of a Gaussian decay, typical of thermal plasmas. These distributions are frequently modelled by the so-called *Kappa* velocity distribution functions and the recent compilations 43 and 44 contain a comprehensive discussion on the properties of Kappa plasmas.

Hence, the propagation and interaction dynamics of waves in dusty Kappa plasmas can be an important research topic regarding particle and energy transport in dust-rich environments, such as planetary rings, magnetospheres of gas giants, star nebulae and the stellar winds of carbon-type stars. Notwithstanding the potential importance, relatively few contributions can be found in the literature investigating the propagation and absorption/amplification of electrostatic/electromagnetic waves in dusty Kappa plasmas.<sup>45–53</sup>

In the first paper (hereafter called Paper I),<sup>54</sup> we investigated the case where the plasma particles are described by standard Kappa distributions, both isotropic and anisotropic. In the case of anisotropic distributions, we have considered the bi-Kappa and product-bi-Kappa models. In the present paper (Paper II), we will consider plasma particles described by *regularized* Kappa distributions, which are categorized below. As far as we are aware, this is the first time that such systematic study is reported in the literature.

The plan of the paper is as follows. In section II the charge-equilibrium equation is briefly derived from the orbital motion limited (OML) theory. In section III the regularized Kappa velocity distribution function is introduced and some of its properties are discussed. In section IV the charge-equilibrium equation is solved for the two different models of the regularized distribution considered in this Paper. The results are presented and analyzed in section V, and in section VI our conclusions are drawn.

## II. THE CHARGE EQUILIBRIUM EQUATION

We consider a spherical dust grain with radius  $a$  immersed in a thermal plasma, which acquires a variable charge  $q(t)$  uniformly distributed over its surface. As mentioned in the Introduction, in this series of two Papers we consider only the collisional charging mechanism; hence, the dust charge equation is simply  $dq/dt = I_0(q)$ , where  $I_0(q)$  is the net current on the surface of the grain when the charge is  $q$ .

Inside the heliosphere, the dust is composed by different materials and has a distribution of sizes that usually follows a power law.<sup>11,55,56</sup> Moreover, interplane-

tary and interstellar dust can also be composed by irregularly shaped aggregates which could accumulate a large charge-to-mass ratio due to its porous nature.<sup>57</sup> In the present Paper, we will assume for simplicity that all grains are spherical with the same radius. Hence, the charging current  $I_0(q)$  is given, in the nonrelativistic limit, by the integration in velocity space<sup>25</sup>

$$I_0(q) = \sum_{\beta} q_{\beta} \int d^3v v \sigma_{\beta}(q, v) f_{\beta 0}(\mathbf{v}),$$

where the summation is performed over the plasma species ( $\beta = e, i, \dots$ ),  $\sigma_{\beta}(q, p)$  is the cross section for dust charging, obtained from the OML theory,<sup>58</sup> given by

$$\sigma_{\beta}(q, v) = \pi a^2 \left( 1 - \frac{2qq_{\beta}}{m_{\beta}av^2} \right) H \left( 1 - \frac{2qq_{\beta}}{m_{\beta}av^2} \right),$$

where  $H(x)$  is the Heaviside function and where  $f_{\beta 0}(\mathbf{v})$ , the velocity distribution function for the  $\beta$ -species, is normalized to its number density  $n_{\beta 0}$  as

$$\int d^3v f_{\beta 0}(\mathbf{v}) = n_{\beta 0}.$$

Moreover,  $q_{\beta}$  and  $m_{\beta}$  are, respectively, the electric charge and the mass of the  $\beta$ -species particle. The dust grains are assumed to be all spherical with radius  $a$ .

The OML theory assumes that the plasma particles move in the vicinity of an immovable grain with a dynamic charge  $q$  along collisionless orbits that satisfy the conservation of mechanical energy and angular momentum, similar to Rutherford scattering.<sup>55,58,59</sup> Usually, the plasma is assumed to be in a local (quasi-) stationary state in such a way that the static VDF  $f_{\beta 0}(\mathbf{v})$  can be employed to describe the collisional charging throughout the dynamical evolution of the charge. Moreover, the effect of the ambient magnetic field is neglected.

Although it is possible to include both the effects of the magnetic field and of the plasma fluctuations in the collisional charging process,<sup>60</sup> we will employ the simpler OML approximation. Ref. 61 developed a generalization of the OML theory including magnetic field and concluded that the traditional approach is valid for a magnetized plasma as long as the dust radius is much smaller than the electron Larmor radius. For the physical parameters considered in this work, this condition is always satisfied. More recent particle simulations<sup>18,62</sup> have corroborated this conclusion and shown that although the total charging time can diminish with the field intensity, the equilibrium charge varies with the magnetic field around an average value, depending on the plasma and dust conditions.

The equilibrium condition for the dust-plasma system is obtained by assuming vanishing charging current over the dust particles. The charging time (the time for the grain to reach the equilibrium charge) for interplanetary and interstellar dust can vary from a few seconds to months depending on the grain composition and radius and its position inside the heliosphere.<sup>11,12,55–57</sup> In

this work, we will assume that the dust grain is fully charged. We denote by  $q_{d0} = -Z_d e$  the dust charge at the equilibrium, where  $Z_d$  is the dust charge number and  $e$  is the elementary charge. In the vast majority of cases,  $Z_d > 0$ , meaning that the dust is negatively charged due to collisions with plasma particles. However, we will show below that under certain circumstances, the dust can become positively charged (*i.e.*,  $Z_d < 0$ ) when immersed in a suprathermal plasma.

The average collision frequency for collisional charging at the equilibrium is then given by<sup>25</sup>

$$\nu_{\beta d} = \frac{n_{d0}}{n_{\beta 0}} \int d^3v v \sigma_{\beta}(q_{d0}, v) f_{\beta 0}(v), \quad (1)$$

where  $n_{d0}$  is the number density of dust grains. Hence, the condition of zero current on the surface of the dust particle,  $I_0(q_{d0} = -Z_d e) = 0$ , can be written as

$$\sum_{\beta} n_{\beta 0} q_{\beta} \nu_{\beta d} = 0.$$

We must also take into account the charge neutrality condition

$$\sum_{\beta} n_{\beta 0} q_{\beta} + n_{d0} q_{d0} = 0.$$

Considering now an electron-ion plasma with dust, where the ion charge is  $q_i = Z e$  ( $Z = 1, 2, \dots$ ), the charge neutrality can be written as  $Z n_{i0} - n_{e0} - Z_d n_{d0} = 0$ . In this case, the zero-current condition results

$$Z \nu_{id}(Z_d) - \left( Z - Z_d \frac{n_{d0}}{n_{i0}} \right) \nu_{ed}(Z_d) = 0. \quad (2)$$

The solution of (2) provides the dust charge number  $Z_d$  at equilibrium.

### III. THE $\kappa$ -REGULARIZED VELOCITY DISTRIBUTION FUNCTION

Space and astrophysical plasmas are frequently observed (or inferred) to be in a (quasi-) stationary turbulent state that is far from the thermal equilibrium. When the plasma is in the equilibrium state, the velocity distribution functions of the particle components are the well-known Maxwell-Boltzmann distributions (the Maxwellian).

On the other hand, direct observations performed by space probes in planetary magnetospheres and in the solar wind have shown that when the plasma is in the stationary turbulent state, the measured VDFs are endowed with distinct non-Maxwellian features, particularly with high-energy tails that follow a power-law dependence on velocity, instead of the Gaussian decay of a Maxwellian. Due to this particular nonthermal feature, remarked since the late 1960s in the plasma of Earth's magnetosphere, the VDFs of space plasmas have been since then modelled

by *Lorentzian* or, more recently, by the *Kappa* distribution functions.<sup>43,44</sup> Plasmas in this particular nonthermal equilibrium state are often referred to in the literature as *suprathermal* or *suprathermal* plasmas. In this work, we will employ the latter denomination throughout.

The first model of a Kappa VDF to appear in a journal publication was introduced by Ref. 63. Over the years, the mathematical forms of Kappa VDFs have acquired several different versions (called here *models*) and the physically correct version is still a matter of controversy in the literature.<sup>43,44,64-67</sup> Most of the different models proposed in the literature can be written in a generalized form introduced by Refs. 68 and 69 and which corresponds to the isotropic version of the distributions employed in Paper I,

$$f_{w,\alpha}(v) = \frac{n_0}{\pi^{3/2} w^3} \frac{\kappa^{-3/2} \Gamma(\sigma)}{\Gamma(\sigma - 3/2)} \left( 1 + \frac{v^2}{\kappa w^2} \right)^{-\sigma}, \quad (3)$$

where  $\Gamma(z)$  is the Gamma function,<sup>70</sup>  $\sigma = \kappa + \alpha$ , with  $\kappa$  being the kappa index that gives the VDF its name and  $\alpha > 0$  is a free parameter (usually integer). The quantity  $w = w(\kappa)$  has the dimension of velocity. Choosing different values and mathematical forms for  $\alpha$  and  $w(\kappa)$ , different models found in the literature can be reproduced by (3), which will be called here the *standard Kappa distribution* (SKD).

Since the initial proposal, the Kappa distribution (3), with particular values for the parameters  $\alpha$  and  $w$ , and its anisotropic generalization, the bi-kappa distribution function,<sup>71</sup> have been consistently employed to fit observed VDFs and other related physical quantities in various space ambients, such as the solar wind.<sup>72-76</sup> The SKD was also employed to estimate the evolution of the proton temperature and the spectral index of energy distribution of energetic neutral atoms (ENAs) in the inner heliosheath from sky maps observed by the Interstellar Boundary Explorer spacecraft.<sup>77</sup>

Notwithstanding the frequent use of the SKD model to interpret observed space and astrophysical data, some inconsistencies have been noticed, both in the observational and theoretical fronts. One important restriction of the SKD is that it can only be defined for  $\sigma > 3/2$  and higher-order moments of (3) impose even more restrictive conditions. For instance, the second moment, which measures the dispersion of particle velocities around the mean, and hence is related to the concept of the temperature of the plasma species, only exists for  $\sigma > 5/2$ . For values of  $\sigma$  below these constraints the VDF moments diverge. Such drawbacks of the SKD have created difficulties for certain applications of the model, such as an hydrodynamic formulation of a Kappa plasma or small-Larmor-radius expansions to study the dynamics of kinetic Alfvén waves.<sup>44,68</sup>

One observational inconsistency is clearly shown by the energy spectral index of the ENAs in the heliosheath. Using the SKD distribution (with  $\alpha = 1$ ) to fit the observed energy distribution, the spectral index agrees with the measured value of the kappa index only for  $\kappa > 3/2$ .

For smaller values the values disagree because the mean kinetic energy derived from the SKD is not defined for  $\kappa < 3/2$ .<sup>77</sup>

In order to correct these deficiencies and find a divergence-free formulation for a suprathermal plasma, a recent model for a nonequilibrium stationary VDF that is valid for any  $\kappa > 0$  and contains all the moments of the distribution, the  $\kappa$ -regularized velocity distribution function (RKD), was proposed initially by Ref. 66 and was later cast in a more generalized form by Ref. 78. Here we will employ the notation introduced by Ref. 79 for the generalized isotropic RKD, given by

$$f_{\kappa,\theta}^{(\eta,\zeta,\mu)}(v) = n_0 N_{\kappa,\theta}^{(\eta,\zeta,\mu)} \left(1 + \frac{v^2}{\eta\theta^2}\right)^{-\zeta} e^{-\mu v^2/\theta^2},$$

where

$$\begin{aligned} \frac{1}{N_{\kappa,\theta}^{(\eta,\zeta,\mu)}} &= (\pi\eta)^{3/2} \theta^3 U\left(\frac{3}{2}, \frac{5}{2} - \zeta, \mu\eta\right) \\ &= \left(\frac{\pi}{\mu}\right)^{3/2} (\mu\eta)^\zeta \theta^3 U\left(\zeta, \zeta - \frac{1}{2}, \mu\eta\right) \end{aligned}$$

is the normalization constant and  $U(a, b, z)$  is one of the solutions of Kummer's equation<sup>80</sup> (also known as the Tricomi function).

The distribution  $f_{\kappa,\theta}^{(\eta,\zeta,\mu)}(v)$  contains the free dimensionless parameters  $\eta = \eta(\kappa)$ ,  $\zeta = \zeta(\kappa)$ , and  $\mu = \mu(\kappa)$ , which must be such that the RKD exists for  $\kappa > 0$ , and also  $\theta = \theta(\kappa)$ , which must be related to the second moment of the distribution via some form of “thermal” velocity and have the dimension of velocity.

Notice that all free parameters can be functions of the kappa index, with the proviso that the usual limit  $\kappa \rightarrow \infty$  must necessarily recover the Maxwellian. Other limits may also reproduce other model VDFs employed in the literature. Finally, the quantity  $\mu(\kappa)$  is called the *regularization parameter* and it is assumed that  $0 \leq \mu \ll 1$ , in such a way that the RKD reduces to the SKD in the limit  $\mu = 0$  and is close to the latter in the low- and medium-energy ranges. It is only in the very-high-energy range that the effect of the Gaussian kicks in and regularizes the distribution. The value of  $\mu$  can also be judiciously chosen so as to minimize the effects of nonphysical super-relativistic particles in a nonrelativistic formulation or numerical simulation.

Since the original proposition, the RKD has been applied to reevaluations of transport coefficients,<sup>81</sup> solar wind observations,<sup>82,83</sup> Harris current sheet,<sup>84</sup> and dusty plasmas.<sup>85</sup>

It is also important to remark here that the RKD is not merely a mathematical model. It was shown that the  $\kappa$ -regularized distribution restores the property of additivity of the Boltzmann-Gibbs entropy formula for a continuous system<sup>67</sup> and that the RKD is a self-consistent solution for the quasi-equilibrium state between Langmuir fluctuations and suprathermal electrons.<sup>86,87</sup>

With the previous observations in mind, we will adopt hereafter the expressions

$$\eta = \kappa, \quad \zeta = \sigma, \quad \sigma = \kappa + \alpha, \quad \mu = \mu_0 \operatorname{sech}\left(\frac{\kappa}{\kappa_0}\right),$$

where  $\{\alpha, \mu_0, \kappa_0\}$  are new free parameters ( $\mu_0 \ll 1$ ), and write  $f_{\kappa,\theta}^{(\kappa,\sigma,\mu)}(v) \equiv f_{\kappa,\theta}^{(\alpha)}(v)$ , where

$$f_{\kappa,\theta}^{(\alpha)}(v) = n_0 N_{\kappa,\theta}^{(\kappa,\sigma,\mu)} \left(1 + \frac{v^2}{\kappa\theta^2}\right)^{-\sigma} e^{-\mu v^2/\theta^2}, \quad (4)$$

and where

$$\begin{aligned} \frac{1}{N_{\kappa,\theta}^{(\kappa,\sigma,\mu)}} &= (\pi\kappa)^{3/2} \theta^3 U\left(\frac{3}{2}, \frac{5}{2} - \sigma, \mu\kappa\right) \\ &= \left(\frac{\pi}{\mu}\right)^{3/2} (\mu\kappa)^\sigma \theta^3 U\left(\sigma, \sigma - \frac{1}{2}, \mu\kappa\right). \end{aligned}$$

The particular form adopted for the RKD in (4) is still sufficiently general to encompass several different models. For instance, setting the regularization parameter  $\mu_0 = 0$  and calling  $\theta(\kappa) = w(\kappa)$ , the RKD reduces to (3). Here, the normalization constant  $N_{\kappa,\theta}^{(\kappa,\sigma,\mu)}$  reduces to the expression in (3) by applying the limiting cases for the Tricomi function discussed in Appendix A.

On the other hand, in the limit  $\kappa \rightarrow \infty$  the RKD transitions smoothly to the Maxwellian,

$$\lim_{\kappa \rightarrow \infty} f_{\kappa,\theta}^{(\alpha)}(v) = f_M(v) = n_0 \frac{e^{-v^2/v_T^2}}{\pi^{3/2} v_T^3}.$$

In order to obtain this limit, one must first notice that  $\kappa\mu(\kappa) \xrightarrow{\kappa \rightarrow \infty} 0$ , employ the Stirling formula for the Gamma functions<sup>70</sup> and the exponential limit  $(1 + y^2/\kappa)^{-\kappa} \xrightarrow{\kappa \rightarrow \infty} e^{-y^2}$ . Moreover, the quantity  $\theta(\kappa)$  must be such that

$$\lim_{\kappa \rightarrow \infty} \theta(\kappa) = \lim_{\kappa \rightarrow \infty} w(\kappa) = v_T = \sqrt{\frac{2T}{m}},$$

where  $v_T$  is the thermal velocity and the temperature is evaluated in energy units.

The explicit expressions for the parameter  $\theta(\kappa)$ , or  $w(\kappa)$ , will be given by two different models, the same models considered by Paper I and which will be discussed below. These models are concerned with the measure of the second moment of the RKD and by the definition of the “temperature” of a suprathermal plasma.

The kinetic temperature obtained from a generic VDF is

$$T_K = \frac{1}{3} m \langle v^2 \rangle,$$

where

$$\langle v^2 \rangle = \frac{1}{n_0} \int d^3v v^2 f_{\alpha 0}(v)$$



is the second moment of the distribution.

Evaluating  $T_K$  from the SKD (3), we obtain

$$T_K = \frac{1}{2} m \frac{\kappa w^2}{\kappa + \alpha - 5/2}, \quad (5)$$

which shows that a physically relevant expression for the kinetic temperature can only be obtained for  $\kappa + \alpha > 5/2$ .

For one of the most employed models, the kinetic temperature is defined in such a way that it is the same measure of the second moment, regardless of the particular value of the  $\kappa$  index. The idea is that the temperature is a measure of the thermality of the stationary system and it must be the same regardless whether the system is in thermal equilibrium or in a nonequilibrium steady state. In this way, independent measures of the temperature, either as the second moment of the VDF or as an intensive parameter obtained from the entropy of a nonequilibrium system are the same and can be considered as a “physical” temperature.<sup>43,88</sup>

For this model, it has been shown<sup>43,88</sup> that using the SKD (3) with  $\alpha = 1$  and  $w^2(\kappa) = (\kappa - 3/2) v_T^2/\kappa$ , there results that  $T = T_K$ . Moreover, the Kappa distribution in this model maximizes the Tsallis entropy  $S_\kappa$  (in terms of the  $\kappa$  index) within the constraints of a canonical ensemble and, consequently, can be evaluated also as  $T^{-1} = \partial S_\kappa / \partial E$ , where  $E$  is the internal energy of the system. More recently, the concept of “entropy deficiency” has been proposed, based on the additivity formula satisfied by the Tsallis entropy,  $S_{A+B} = S_A + S_B - \kappa^{-1} S_A S_B$ , where  $A$  and  $B$  are two independent statistical systems.<sup>89,90</sup> Using this concept, it was shown that this form of the SKD is the only one that can satisfy Tsallis’s additivity formula.<sup>91</sup>

This model is completely self-consistent with Tsallis’s entropic principle of nonadditive, nonequilibrium statistical mechanics and, for this reason, has been extensively employed in the literature.<sup>43</sup>

For the other model considered in this work, the parameter  $w$  in (3) is a constant, given by  $w^2 = 2T_\kappa/m$ , where  $T_\kappa$  is some measure of the second moment.<sup>63,92</sup> In this case, the kinetic temperature (5) becomes kappa-dependent. This form of the SKD is sometimes called “Olbertian” and has also been extensively used (usually with  $\alpha = 1$ ) in the literature,<sup>44,93–96</sup> since clear correlations of the measured temperature (and related parameters) of the plasma species with the measured kappa index were found in the solar wind,<sup>93</sup> the Earth’s magnetosphere,<sup>94,95</sup> and in the inner heliosheath.<sup>77</sup>

One of the objectives of this Paper II is to analyse the differences on the charging of the dust grains using both interpretations of the kinetic temperature, but now for the regularized Kappa distribution. Accordingly, evaluating now  $\langle v^2 \rangle$  with the RKD  $f_{\kappa,\theta}^{(\alpha)}(v)$  given by (4), we arrive at the integral

$$\langle v^2 \rangle = 4\pi N_{\kappa,\theta}^{(\kappa,\sigma,\mu)} \int_0^\infty dv v^4 \left( 1 + \frac{v^2}{\kappa\theta^2} \right)^{-\sigma} e^{-\mu v^2/\theta^2}.$$

Upon defining the new integration variable  $t = v^2/\kappa\theta^2$ , we can identify the integral identity (A2) and then obtain

$$\langle v^2 \rangle = \frac{3}{2} \mu^{-1} \frac{U(\sigma, \sigma - 3/2, \mu\kappa)}{U(\sigma, \sigma - 1/2, \mu\kappa)} \theta^2,$$

where we have also used the Kummer identity (A3).

A more compact notation can be achieved if we introduce the symbols

$$[m]\mathcal{U}^{[n]}(\eta, \zeta, \mu) = \frac{(\mu\eta)^{-m/2} U(\zeta, \zeta - \frac{1+m}{2}, \mu\eta)}{(\mu\eta)^{-n/2} U(\zeta, \zeta - \frac{1+n}{2}, \mu\eta)}, \quad (6a)$$

$$[m]\mathcal{U}(\eta, \zeta, \mu) = [m]\mathcal{U}^{[0]}(\eta, \zeta, \mu),$$

$$\mathcal{U}^{[n]}(\eta, \zeta, \mu) = [0]\mathcal{U}^{[n]}(\eta, \zeta, \mu),$$

which were originally defined by Ref. 78. In this work, we also introduce the symbol

$$[m]\mathcal{U}_d(\eta, \zeta, \mu, \chi) = \frac{U(\zeta, \zeta - \frac{1+m}{2}, \mu\eta(1 + \chi/\eta))}{(\mu\eta)^{m/2} U(\zeta, \zeta - \frac{1}{2}, \mu\eta)} e^{-\mu\chi}, \quad (6b)$$

which is the dusty plasma counterpart to  $[m]\mathcal{U}(\eta, \zeta, \mu)$ . Obviously,  $[m]\mathcal{U}_d(\eta, \zeta, \mu, 0) = [m]\mathcal{U}(\eta, \zeta, \mu)$ .

Therefore, the kinetic temperature for a RKD plasma can be written as

$$T_K = \frac{1}{2} m \kappa [2]\mathcal{U}(\kappa, \kappa + \alpha, \mu) \theta^2. \quad (7)$$

The expression for the kinetic temperature given by (7) is important for the following discussion concerning the models adopted in this work.

#### IV. THE CHARGING OF DUST GRAINS WITH DIFFERENT RKD MODELS

The dust charge equilibrium equation (2) will be solved for two different models of the  $\kappa$ -regularized velocity distribution function. We will first obtain a general expression for the collision frequencies (1) of the dust grains in a electron-ion plasma whose velocity distribution functions are given by the generalized form (4).

##### A. The general form of the collision frequencies

As the results will show, in extreme cases of suprathermality the dust grains can acquire a positive net charge, although the charge will be negative for the vast majority of the cases. Because of this possibility, we have to solve the integrations in (1) taking into account both possible charge signs. Inserting then the distribution (4) into (1), we have the collision frequency of the dust grains with the  $\beta$ -th plasma species ( $\beta = e, i$ ) given by

$$\nu_{\beta d} = 4\pi^2 a^2 n_{d0} N_{\kappa_\beta, \theta_\beta}^{(\kappa_\beta, \sigma_\beta, \mu_\beta)} \int_0^\infty dv v (v^2 - V_\beta^2)$$

$$\times H(v^2 - V_\beta^2) \left(1 + \frac{v^2}{\kappa_\beta \theta_\beta^2}\right)^{-\sigma_\beta} e^{-\mu_\beta v^2 / \theta_\beta^2},$$

where we have defined the constant

$$V_\beta^2 = \frac{2q_{d0}q_\beta}{m_\beta a},$$

which would correspond to the square of the velocity acquired at infinity by a  $\beta$ -species particle initially at rest at the surface of a dust grain with charge  $q_{d0}$  and radius  $a$ , if  $q_{d0}q_\beta > 0$ . Here,  $V_\beta^2$  is just convenient definition for a real constant that can have either positive or negative signs.

Now we have to consider the 2 possible signs of  $V_\beta^2$  separately.

$V_\beta^2 < 0$ . In this case, we write  $V_\beta^2 = |V_\beta^2|$  and obtain

$$\nu_{\beta d} = 4\pi^2 a^2 n_{d0} N_{\kappa_\beta, \theta_\beta}^{(\kappa_\beta, \sigma_\beta, \mu_\beta)} \left( I^{(1)} + V_\beta^2 I^{(0)} \right),$$

where

$$I^{(\ell)} = \int_0^\infty dv v^{2\ell+1} \left(1 + \frac{v^2}{\kappa_\beta \theta_\beta^2}\right)^{-\sigma_\beta} e^{-\mu_\beta v^2 / \theta_\beta^2}.$$

The collision frequencies for a species/population whose VDF is a RKD can be cast in a single expression from the results above as

$$\nu_{\beta d}^{(\kappa_\beta, \alpha_\beta, \mu_\beta)} = 2\sqrt{\pi} a^2 n_{d0} \kappa_\beta^{1/2} \theta_\beta \times \begin{cases} [^{1}] \mathcal{U}(\kappa_\beta, \sigma_\beta, \mu_\beta) + [^{-1}] \mathcal{U}(\kappa_\beta, \sigma_\beta, \mu_\beta) \frac{|V_\beta^2|}{\kappa_\beta \theta_\beta^2}, & q_{d0}q_\beta < 0 \\ [^{1}] \mathcal{U}_d\left(\kappa_\beta, \sigma_\beta, \mu_\beta, \frac{V_\beta^2}{\theta_\beta^2}\right), & q_{d0}q_\beta \geq 0, \end{cases} \quad (8a)$$

in terms of the symbols defined in (6a, b).

In the limit  $\mu_{\beta 0} \rightarrow 0$ , employing again the limiting properties shown in the Appendix, we have, for  $\sigma_\beta > 5/2$  and  $\theta_\beta = w_\beta$ , the collision frequencies for a SKD plasma,

$$\nu_{\beta d}^{(\kappa_\beta, \alpha_\beta)} = 2\sqrt{\pi} a^2 n_{d0} w_\beta \frac{\kappa_\beta^{1/2} \Gamma(\sigma_\beta - 2)}{\Gamma(\sigma_\beta - 3/2)} \times \begin{cases} 1 + \frac{\sigma_\beta - 2}{\kappa_\beta} \frac{|V_\beta^2|}{w_\beta^2}, & q_{d0}q_\beta < 0 \\ \left(1 + \frac{1}{\kappa_\beta} \frac{V_\beta^2}{w_\beta^2}\right)^{-(\sigma_\beta - 2)}, & q_{d0}q_\beta \geq 0, \end{cases} \quad (8b)$$

which correspond to the isotropic limit of the models considered in Paper I.

Finally, in the limit  $\kappa_\beta \rightarrow \infty$ , we have  $\mu_\beta \kappa_\beta \rightarrow 0$ ,  $w_\beta = v_{T\beta}$  and then we obtain the collision frequencies of

Changing the integration variable to  $v^2 = \kappa_\beta \theta_\beta^2 t$ , we employ again identities (A2) and (A3) and obtain

$$\nu_{\beta d}^{(\text{RKD})} = 2\pi^2 a^2 n_{d0} \kappa_\beta^{\sigma_\beta} \theta_\beta^2 \mu_\beta^{\sigma_\beta - 1} N_{\kappa_\beta, \theta_\beta}^{(\kappa_\beta, \sigma_\beta, \mu_\beta)} \times \left[ \theta_\beta^2 \mu_\beta^{-1} U(\sigma_\beta, \sigma_\beta - 1, \mu_\beta \kappa_\beta) + \mathcal{V}_\beta^2 U(\sigma_\beta, \sigma_\beta, \mu_\beta \kappa_\beta) \right].$$

$V_\beta^2 \geq 0$ . In this case, starting with

$$\nu_{\beta d} = 4\pi^2 a^2 n_{d0} N_{\kappa_\beta, \theta_\beta}^{(\kappa_\beta, \sigma_\beta, \mu_\beta)} \times \int_{V_\beta}^\infty dv v (v^2 - V_\beta^2) \left(1 + \frac{v^2}{\kappa_\beta \theta_\beta^2}\right)^{-\sigma_\beta} e^{-\mu_\beta v^2 / \theta_\beta^2},$$

we define the new integration variable

$$v^2 = \kappa_\beta \theta_\beta^2 (\psi_\beta t + E_\beta),$$

where

$$E_\beta = \frac{V_\beta^2}{\kappa_\beta \theta_\beta^2}, \quad \psi_\beta = 1 + E_\beta,$$

and then we obtain

$$\nu_{\beta d}^{(\text{RKD})} = 2\pi^2 a^2 n_{d0} N_{\kappa_\beta, \theta_\beta}^{(\kappa_\beta, \sigma_\beta, \mu_\beta)} (\kappa_\beta \theta_\beta^2)^2 (\mu_\beta \kappa_\beta)^{\sigma_\beta - 2} \times e^{-\mu_\beta V_\beta^2 / \theta_\beta^2} U\left(\sigma_\beta, \sigma_\beta - 1, \mu_\beta \kappa_\beta \left(1 + \frac{V_\beta^2}{\kappa_\beta \theta_\beta^2}\right)\right).$$

dust with Maxwellian particles,

$$\nu_{\beta d}^{(\text{M})} = 2\sqrt{\pi} a^2 n_{d0} v_{T\beta} \times \begin{cases} 1 + \frac{|V_\beta^2|}{v_{T\beta}^2}, & q_{d0}q_\beta < 0 \\ e^{-V_\beta^2 / v_{T\beta}^2}, & q_{d0}q_\beta \geq 0. \end{cases} \quad (8c)$$

We can now propose the following relations and nondimensional quantities to be used by both models,

$$\tilde{a} = \frac{a}{\lambda_i}, \quad \epsilon = \frac{n_{d0}}{n_{i0}}, \quad \tau_e = \frac{T_e}{T_i}, \quad \chi_e = \frac{Z_d e^2}{a T_e} = \frac{Z_d}{\tau_e \tilde{a}},$$

$$v_{Ti}^2 = v_A^2 \beta_i, \quad v_{Te}^2 = \frac{m_i}{m_e} \tau_e v_A^2 \beta_i, \quad \gamma = \frac{\lambda_i^2 n_{i0} v_A}{\Omega_i},$$

where

$$\lambda_i = \frac{e^2}{T_i}, \quad \beta_i = \frac{8\pi n_{i0} T_i}{B_0^2},$$

$$v_A = \frac{B_0}{\sqrt{4\pi n_{i0} m_i}}, \quad \Omega_i = \frac{ZeB_0}{m_i c},$$

are, respectively, the classical distance of minimum approach for ions, the beta parameter for ions, the Alfvén speed and the ion (angular) cyclotron frequency.

Now the general form for the collision frequency  $\nu_{\beta d}$  will be first written in terms of a normalized frequency  $\tilde{\nu}_{\beta d}$ , as  $\nu_{\beta d} = \Omega_i \tilde{\nu}_{\beta d}$ , which in turn will be written in

terms of a collision frequency factor  $\hat{\nu}_{\beta d}$ , where

$$\tilde{\nu}_{\beta d} = C \hat{\nu}_{\beta d}, \quad C = 2\sqrt{\pi} \gamma \epsilon \tilde{a}^2 \beta_i^{1/2}.$$

In this way, the equilibrium charge equation (2) can be written as an equation for the normalized potential  $\chi_e$  in terms of the frequency factors as

$$(Z - \tilde{a} \tau_e \epsilon \chi_e) \hat{\nu}_{ed}(\chi_e) - Z \hat{\nu}_{id}(\chi_e) = 0, \quad (9)$$

where expressions for the collision frequencies from different VDF models can be introduced.

## B. Model 1. Kappa-dependent temperature

The first model to be considered for the RKD assumes that the parameter  $\theta$  for the  $\beta$ -species is a constant, given by  $\theta_\beta^2 = v_{T\beta}^2 = 2T_\beta/m_\beta$ , where  $T_\beta$  is a measure of the second moment of the VDF. With this model, the kinetic temperature given by (7) is not  $\kappa$ -invariant. In fact,

$$T_K(\kappa) = \kappa^{[2]} \mathcal{U}(\kappa, \sigma, \mu) T.$$

In this model, the collision factors for a RKD plasma, from (8a), become

$$\hat{\nu}_{id}^{(\kappa_i, \alpha_i, \mu_i)} = \kappa_i^{1/2} \times \begin{cases} [1] \mathcal{U}(\kappa_i, \sigma_i, \mu_i) + Z \frac{\tau_e \chi_e}{\kappa_i} [-1] \mathcal{U}(\kappa_i, \sigma_i, \mu_i), & \chi_e \geq 0 \\ [1] \mathcal{U}_d(\kappa_i, \sigma_i, \mu_i, -Z \tau_e \chi_e), & \chi_e < 0 \end{cases} \quad (10a)$$

$$\hat{\nu}_{ed}^{(\kappa_e, \alpha_e, \mu_e)} = \sqrt{\frac{m_i}{m_e} \tau_e \kappa_e} \times \begin{cases} [1] \mathcal{U}_d(\kappa_e, \sigma_e, \mu_e, \chi_e), & \chi_e \geq 0 \\ [1] \mathcal{U}(\kappa_e, \sigma_e, \mu_e) - \frac{\chi_e}{\kappa_e} [-1] \mathcal{U}(\kappa_e, \sigma_e, \mu_e), & \chi_e < 0. \end{cases} \quad (10b)$$

We will also need the collision factors for a Maxwellian plasma, which will be given from (8c) as

$$\hat{\nu}_{id}^{(M)} = \begin{cases} 1 + Z \tau_e \chi_e, & \chi_e \geq 0 \\ e^{Z \tau_e \chi_e}, & \chi_e < 0 \end{cases} \quad (11a)$$

$$\hat{\nu}_{ed}^{(M)} = \sqrt{\frac{m_i}{m_e} \tau_e} \times \begin{cases} e^{-\chi_e}, & \chi_e \geq 0 \\ 1 - \chi_e, & \chi_e < 0. \end{cases} \quad (11b)$$

In the next section, expressions (10a, b) or (11a, b), depending on the suprathermality state of either species, will be introduced into the charge equation (9) in order to obtain the equilibrium dust charge for this model.

## C. Model 2. Kappa-invariant temperature

In this model, the kinetic temperature will be evaluated in such a way that is kappa-invariant. If we want the kinetic temperature independent of  $\kappa$  (and also of  $\alpha$

and  $\mu$ ), we must have from (7),

$$T_K = \frac{1}{2} m \kappa^{[2]} \mathcal{U}(\kappa, \kappa + \alpha, \mu) \theta^2 = \frac{1}{2} m v_T^2 = T,$$

where  $T$  is the physical temperature. Therefore, we have the  $\kappa$ -dependent parameter

$$\theta^2(\kappa) = \kappa^{-1} \mathcal{U}^{[2]}(\kappa, \kappa + \alpha, \mu) v_T^2,$$

according to the symmetry property (A1). The quantity  $\theta(\kappa)$  measures the second moment of the RKD in model 2, and on the limit  $\mu_0 \rightarrow 0$  it reduces to the SKD value

$$\theta^2(\kappa) = w^2(\kappa) = \frac{\kappa + \alpha - 5/2}{\kappa} v_T^2,$$

which imposes the constraint  $\kappa + \alpha > 5/2$  on the possible kappa values.

On the other hand, for a plasma species described by the RKD, any  $\kappa > 0$  is possible. However, a  $\kappa$ -invariant

temperature is only meaningful for integer  $\alpha = 0, 1$ , because although  $\langle v^2 \rangle$  exists for any  $\alpha$  and  $\kappa$ , for a finite  $\theta$  we have:

$$\begin{aligned} \alpha = 0 : \quad & \lim_{\kappa \rightarrow 0} \langle v^2 \rangle = \frac{3}{2} \mu_0^{-1} \theta^2 \\ \alpha = 1 : \quad & \lim_{\kappa \rightarrow 0} \langle v^2 \rangle = \frac{1}{2} \mu_0^{-1} \theta^2 \end{aligned}$$

$$\alpha \geq 2 : \quad \lim_{\kappa \rightarrow 0} \langle v^2 \rangle = 0.$$

Hence, for  $\alpha \geq 2$  the second moment is zero and the measure of the physical temperature become meaningless.

Now, for this model, the collision factors (8a) become

$$\hat{\nu}_{id}^{(\kappa_i, \alpha_i, \mu_i)} = \sqrt{\phi_i} \times \begin{cases} [1] \mathcal{U}(\kappa_i, \sigma_i, \mu_i) + Z \frac{\tau_e \chi_e}{\phi_i} [-1] \mathcal{U}(\kappa_i, \sigma_i, \mu_i), & \chi_e \geq 0 \\ [1] \mathcal{U}_d\left(\kappa_i, \sigma_i, \mu_i, -\frac{Z \kappa_i \tau_e}{\phi_i} \chi_e\right), & \chi_e < 0 \end{cases} \quad (12a)$$

$$\hat{\nu}_{ed}^{(\kappa_e, \alpha_e, \mu_e)} = \sqrt{\frac{m_i}{m_e} \tau_e \phi_e} \times \begin{cases} [1] \mathcal{U}_d\left(\kappa_e, \sigma_e, \mu_e, \frac{\kappa_e}{\phi_e} \chi_e\right), & \chi_e \geq 0 \\ [1] \mathcal{U}(\kappa_e, \sigma_e, \mu_e) - \frac{\chi_e}{\phi_e} [-1] \mathcal{U}(\kappa_e, \sigma_e, \mu_e), & \chi_e < 0, \end{cases} \quad (12b)$$

where we have also defined the quantity  $\phi_\beta = \mathcal{U}^{[2]}(\kappa_\beta, \sigma_\beta, \mu_\beta)$ , for brevity.

For this model we can also consider the case where one of the species is Maxwellian, in which case we will employ the factors (11a, b) again.

Some solutions of the charge equation (9), obtained from both models are discussed in the next section.

## V. NUMERICAL SOLUTIONS

Here we will discuss some solutions of the charge equilibrium equation (9). Solutions from each of the models introduced in the previous section will be presented separately.

In order to reduce the quantity of free indices in the analysis, we will restrict ourselves to the particular case  $\alpha_e = \alpha_i = Z = 1$ , with  $m_i/m_e = 1836.152673426$ . Moreover, we will take  $\kappa_0 = 50$ , which will render the parameter  $\mu(\kappa) \approx \mu_0$  for most of the considered cases, and we will also keep the same physical parameters  $a = 10^{-4}$  cm,  $n_{i0} = 10 \text{ cm}^{-3}$ ,  $\epsilon = 10^{-5}$ ,  $\beta_i = 2$ ,  $v_A/c = 10^{-4}$ , and  $\tau_e = 1$  used by Paper I, because we are interested in exploring the effect of suprathermality on the charging process, and these parameters are independent of the suprathermal state of the plasma species. Nevertheless, it is important to point out that these values are typical of stellar winds from carbon-rich stars.<sup>5</sup>

Plots of the solutions of the charge equilibrium equation (9) will be presented for the following cases:

**Case 1:** Ions: Maxwellian ( $\hat{\nu}_{id} = \hat{\nu}_{id}^{(M)}$ ). Electrons: RKD ( $\hat{\nu}_{ed} = \hat{\nu}_{ed}^{(\kappa_e, 1, \mu_e)}$ ).

**Case 2:** Ions: RKD ( $\hat{\nu}_{id} = \hat{\nu}_{id}^{(\kappa_i, 1, \mu_i)}$ ). Electrons: Maxwellian ( $\hat{\nu}_{ed} = \hat{\nu}_{ed}^{(M)}$ ).

**Case 3:** Ions: RKD ( $\hat{\nu}_{id} = \hat{\nu}_{id}^{(\kappa_i, 1, \mu_i)}$ ) (varying  $\kappa_i$ ). Electrons: RKD ( $\hat{\nu}_{ed} = \hat{\nu}_{ed}^{(\kappa_e, 1, \mu_e)}$ ) (fixed  $\kappa_e$ ).

**Case 4:** Ions: RKD ( $\hat{\nu}_{id} = \hat{\nu}_{id}^{(\kappa_i, 1, \mu_i)}$ ) (varying  $\kappa_i$ ). Electrons: RKD ( $\hat{\nu}_{ed} = \hat{\nu}_{ed}^{(\kappa_e, 1, \mu_e)}$ ) (varying  $\kappa_e$ ).

Since the results from the RKD asymptotically approach the results from the SKD as  $\kappa$  grows (because  $\mu(\kappa) \rightarrow 0$ ), most of the results will be restricted to the small-kappa range. The results obtained for large  $\kappa$  are essentially the same as those obtained by the isotropic versions of the SKDs considered in Paper I. In this way, we emphasize the particular behavior of dust charging by extreme suprathermal plasmas.

### A. Model 1

Results from the model 1, introduced in section IV B, are shown here. Figure 1 is an example of solutions of the charge equilibrium equation (9). This plot was obtained considering case 1: Maxwellian ions and RKD electrons, for different values of the regularization parameter  $\mu_{e0}$ , showing the ratio of the dust charge number  $Z_d^{(\text{case1})}$  over the charge number of a fully Maxwellian plasma  $Z_d^{(M)}$ , which is  $Z_d^{(M)} = 15466.77$  for the parameters used.

The results are consistent with the results obtained in Paper I; as  $\kappa_e$  diminishes, the ratio  $Z_d^{(\text{case1})}/Z_d^{(M)}$  grows, due to the excess of suprathermal electrons. However, differently from the SKD results, a RKD plasma supports states with  $\kappa_e < 3/2$ . When  $\kappa_e \lesssim 3/2$  the ratio starts to saturate. This happens because of the cut-off imposed by the regularization parameter  $\mu_0$  that imposes that high-energy particles are essentially Gaussian, although they are still present in greater number than in a Maxwellian



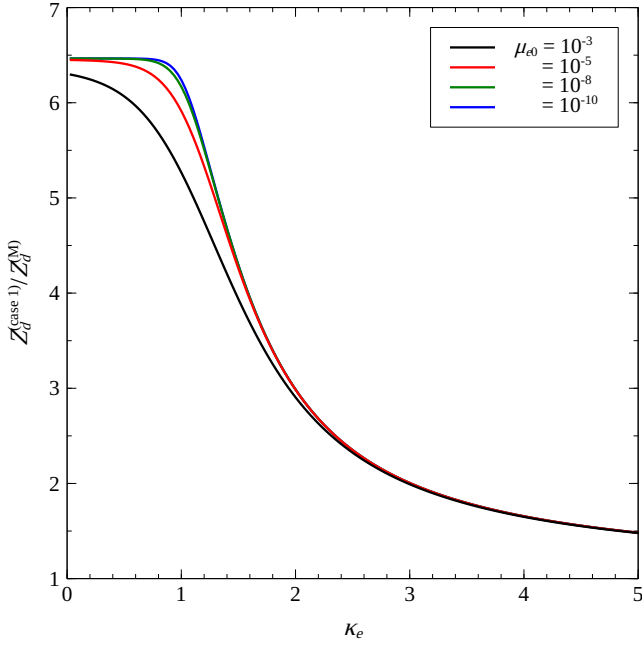


Figure 1. Plots of the charge number ratios  $Z_d^{(\text{case 1})}/Z_d^{(\text{M})}$  for RKD electrons and Maxwellian ions (case 1) as function of  $\kappa_e$ .

plasma. As  $\mu_{e0}$  diminishes, the ratio becomes essentially invariant on the regularization parameter, because the total number of electrons is always the same.

On the other hand, as  $\kappa_e \rightarrow \infty$ , the electronic VDF tends to the Maxwellian and, consequently, the charge number ratio approaches the unity.

The behavior shown by Fig. 1 is in accordance with previous studies about dust charging in suprathermal plasmas when the electrons are suprathermal and the ions are Maxwellian (see, *e.g.*, Ref. 45 or Paper I). The dust charge is enhanced due to the excess of suprathermal electrons, and the charge is always negative.

A different picture emerges when the ions are more suprathermal than the electrons. A recent paper (Ref. 85) has put forth the possibility that in this case the dust charge can become positive (*i.e.*,  $Z_d < 0$ ). The results we have obtained corroborate this conclusion, but with much more stringent conditions than those obtained by Ref. 85.

A comprehensive study on the dust charging process with a electron-ion RKD plasma would in principle demand a complete analysis of the four-dimensional parameter space  $\{\mu_{0e}, \kappa_e, \mu_{0i}, \kappa_i\}$ . However, a few choice cases are sufficient for us to reach the relevant conclusions. Figure 2 shows the charge number ratios for several values of the RKD parameters, corresponding to cases 2 and 3. Continuous lines are obtained for fixed  $\mu_{e0} = 10^{-2}$  and  $\kappa_e = 2$ ; dashed lines for the same  $\mu_{e0}$  and  $\kappa_e = 5$ ; and dotted lines for  $\kappa_e \rightarrow \infty$  (Maxwellian). The color codes correspond to  $\mu_{i0} = 10^{-2}$  (black lines),  $10^{-3}$  (red),  $10^{-4}$  (green),  $5 \times 10^{-5}$  (blue), and  $10^{-5}$  (magenta). All results

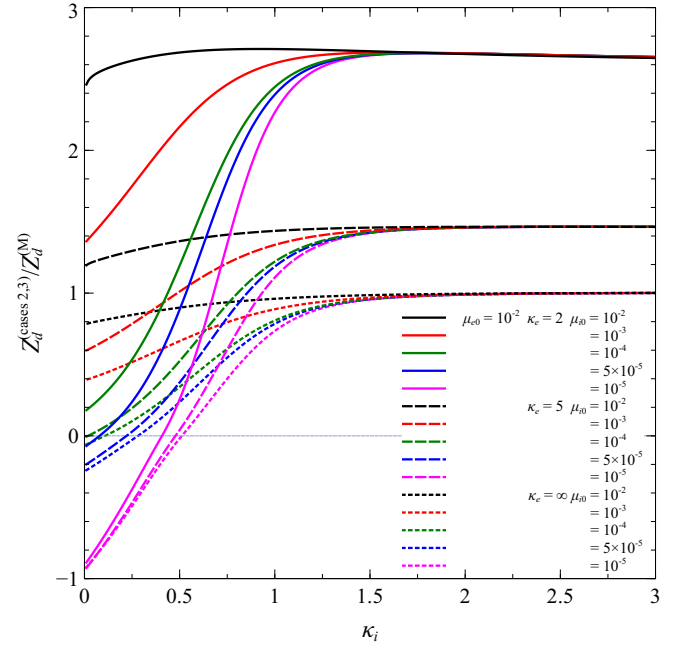


Figure 2. Plots of the charge number ratios  $Z_d^{(\text{cases 2,3})}/Z_d^{(\text{M})}$  for RKD ions and RKD or Maxwellian electrons (cases 2 and 3) as functions of  $\kappa_i$ , for  $\mu_{i0} = 10^{-2}$  (black),  $10^{-3}$  (red),  $10^{-4}$  (green),  $5 \times 10^{-5}$  (blue), and  $10^{-5}$  (magenta). Continuous lines: constant  $\mu_{e0} = 10^{-2}$  and  $\kappa_e = 2$ . Dashed lines: same  $\mu_{e0}$  and  $\kappa_e = 5$ . Dotted lines:  $\kappa_e \rightarrow \infty$  (Maxwellian).

are displayed for the ratios  $Z_d^{(\text{cases 2,3})}/Z_d^{(\text{M})}$  as functions of  $\kappa_i$ .

The first striking behavior displayed in Fig. 2 is that the charge ratio is roughly constant for  $\kappa_i \gtrsim 3/2$  and for any  $\mu_{i0}$ , irrespective to whether the electrons are thermal ( $\kappa_e \rightarrow \infty$ ) or suprathermal ( $\kappa_e = 2$ ). Moreover, the overall behavior is similar to case 1: the dust charge is negative ( $Z_d > 0$ ), with larger charge numbers when the electrons are more suprathermal.

However, as the ion kappa index approaches the regularized region ( $\kappa_i \lesssim 1$ ), the behavior starts to change. The charge ratios split for different values of  $\mu_{i0}$  and generally diminish as  $\kappa_i \rightarrow 0$ , in a opposite trend to that displayed in case 1. When the electrons are very suprathermal ( $\mu_{e0} = 10^{-2}$  and  $\kappa_e = 2$ ), the ratio can still be positive even for  $\kappa_i = 0$ , although with  $Z_d^{(\text{cases 2,3})} < Z_d^{(\text{M})}$  in some extreme cases. In even more extreme cases, one observes the continuous curves crossing the null-charge boundary for very small values of  $\mu_{0i}$  and  $\kappa_i$ . This trend is more pronounced when the electrons are moderately suprathermal ( $\kappa_e = 5$ ) and even more pronounced when the electrons are thermal ( $\kappa_e \rightarrow \infty$ ). In all considered cases, the dust charge ends up positive when  $\mu_{i0} = 10^{-5}$  and  $\kappa_i \approx 0$ , with the upper-level case  $Z_d^{(\text{cases 2,3})} \approx -Z_d^{(\text{M})}$ .

Therefore, the dust charge can indeed become positive when the ions are highly suprathermal. In order to better elucidate this possibility, we will examine the null-charge

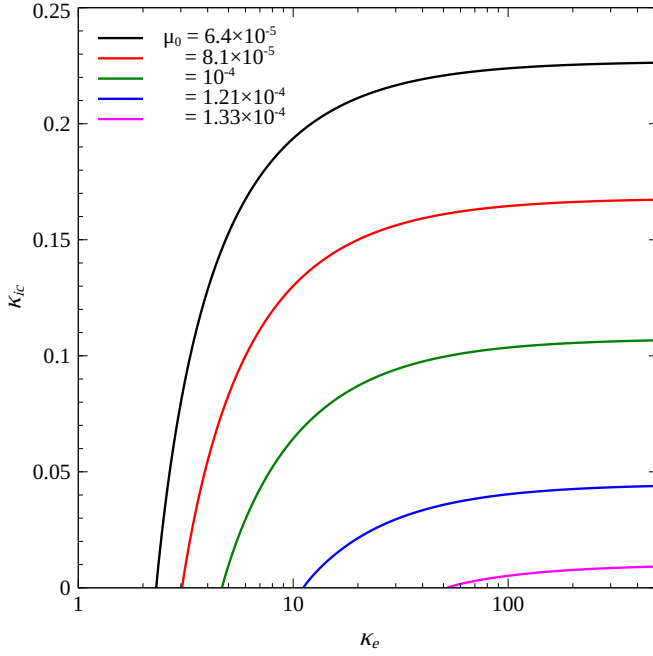


Figure 3. Plots of  $\kappa_{ic}$ , the solution of (13), as a function of  $\kappa_e$ , for several values of  $\mu_{0e} = \mu_{0i} = \mu_0$ .

condition from Eq. (9). Setting  $\chi_e = 0$  and introducing the collision factors (10a, b), the null-charge condition for Model 1 is obtained for a critical  $\kappa_i = \kappa_{ic}$ , given by

$$\sqrt{\kappa_{ic}}^{[1]} \mathcal{U}(\kappa_{ic}, \kappa_{ic} + 1, \mu_i) = \sqrt{\frac{m_i}{m_e} \tau_e \kappa_e}^{[1]} \mathcal{U}(\kappa_e, \kappa_e + 1, \mu_e). \quad (13)$$

Figure 3 shows some values of  $\kappa_{ic}$  as a function of  $\kappa_e$  for several values of the regularization parameter  $\mu_{e0} = \mu_{i0} = \mu_0$ . For any set of RKD parameters, the dust will only acquire a positive charge for  $\kappa_i < \kappa_{ic}$  and, even so, when  $\kappa_e$  is greater than a critical value  $\kappa_{ec} \gg \kappa_{ic}$ . Moreover, the value of  $\kappa_{ec}$  rapidly increases more than an order of magnitude with a relatively smaller increase of  $\mu_0$ .

Fig. 3 considers the range of electron kappa-indices  $1 \leq \kappa_e \leq 500$  and in all considered cases we obtained  $\kappa_{ic} \ll 1$ . Moreover, the results show that for any  $\mu_0$ , the value of  $\kappa_{ic}$  saturates even when the electrons thermalize ( $\kappa_e \rightarrow \infty$ ). The value of the regularization parameter is also crucial, favoring the occurrence of positive dust when  $\mu_0$  is very small, with this possibility disappearing when  $\mu_0 \gtrsim 1.33 \times 10^{-4}$ . This happens because a very small  $\mu_0$  allows for the presence of a substantial number of extremely suprathermal ions for a RKD with  $\kappa_i \ll 1$ .

From these results, one concludes that although positively-charged dust grains are predicted when immersed in a RKD plasma, this can happen only when there is an extreme difference between the suprathermal states of ions and electrons, with the ions necessarily be-

ing much more suprathermal than the electrons; the ionic kappa index must be smaller than  $\kappa_e$  by at least one order of magnitude. These results contrast from those obtained by Ref. 85, which predicted a milder discrepancy in the suprathermal states, when employing the same RKD model.

Such large disparity between the  $\kappa_i$  and  $\kappa_e$  indices, necessary for null-charge, is unlikely to be detected in space and astrophysical systems. Observations performed in the solar wind<sup>74,97,98</sup> measured kappa indices  $\kappa_i \sim \kappa_e \lesssim 5$ , that are roughly of the same order of magnitude for electrons and protons, for a large range of solar radii.

One must also point out that the condition  $\kappa_i \ll \kappa_e$  (with  $\mu_{i0} = \mu_{e0}$ ) for  $Z_d < 0$  was obtained using model 1. In the next section we will present the results from model 2, which are substantially different.

As final results from model 1, figure 4 shows contour plots of the normalized potential  $\chi_e$ , the solution of (9), as a function of  $\kappa_e \times \kappa_i$  for several values of the regularization parameter  $\mu_{i0} = \mu_{e0} = \mu_0$  (this corresponds to case 4: varying  $\kappa_i$  and  $\kappa_e$ ). As a reference, the potential for a fully Maxwellian plasma is  $\chi_e^{(M)} = 2.374$ .

In all considered situations, each panel of Fig. 4 presents regions with either  $\chi_e < 0$  or  $\chi_e > 0$ , with the null-charge condition emphasized with a thicker contour line. In all panels, the region on the left of the  $\chi_e = 0$  line corresponds to positively-charged dust grains, whereas the region on the right denotes negative charges.

The plots on Fig. 4 corroborate the conclusions drawn from the analysis of the behavior of  $\kappa_{ic}$ . For a given value of  $\mu_0$ , positive charge is only possible for  $\kappa_i < \kappa_{ic}$ , when  $\kappa_e > \kappa_{ec}$ , and in all considered situations,  $\kappa_{ec} \gg \kappa_{ic}$  by at least one order of magnitude.

Finally, the largest negative potential (corresponding to positive charge) observed is relatively mild, rarely of the order (in absolute value) of the Maxwellian  $\chi_e^{(M)}$ . On the other hand, all plots show that when  $\kappa_e < \kappa_{ec}$ , the potential grows very fast and becomes much larger than  $\chi_e^{(M)}$  as  $\kappa_e \rightarrow 0$ . At this point, the potential becomes largely independent on the value of  $\kappa_i$ .

Summarizing the results from model 1, the dust charge is still negative in the majority of the 4-dimensional RKD parameter space, with  $Z_d^{(RKD)} \gg Z_d^{(M)}$  whenever the electrons are on the same level of suprathermality than the ions, or higher ( $\kappa_e \lesssim \kappa_i$ ). The occurrence of positively-charged dust grains by the collisions with suprathermal plasma particles is only possible when the ions are on an extreme level of suprathermality compared to the electrons ( $\kappa_i \ll \kappa_e$ ). We believe that the possibility of occurrence of such extreme differences in naturally-occurring environments is highly unlikely and, hence, the collisional charging mechanism alone should mostly still render the dust grains negatively charged, even when the plasma environment is suprathermal.

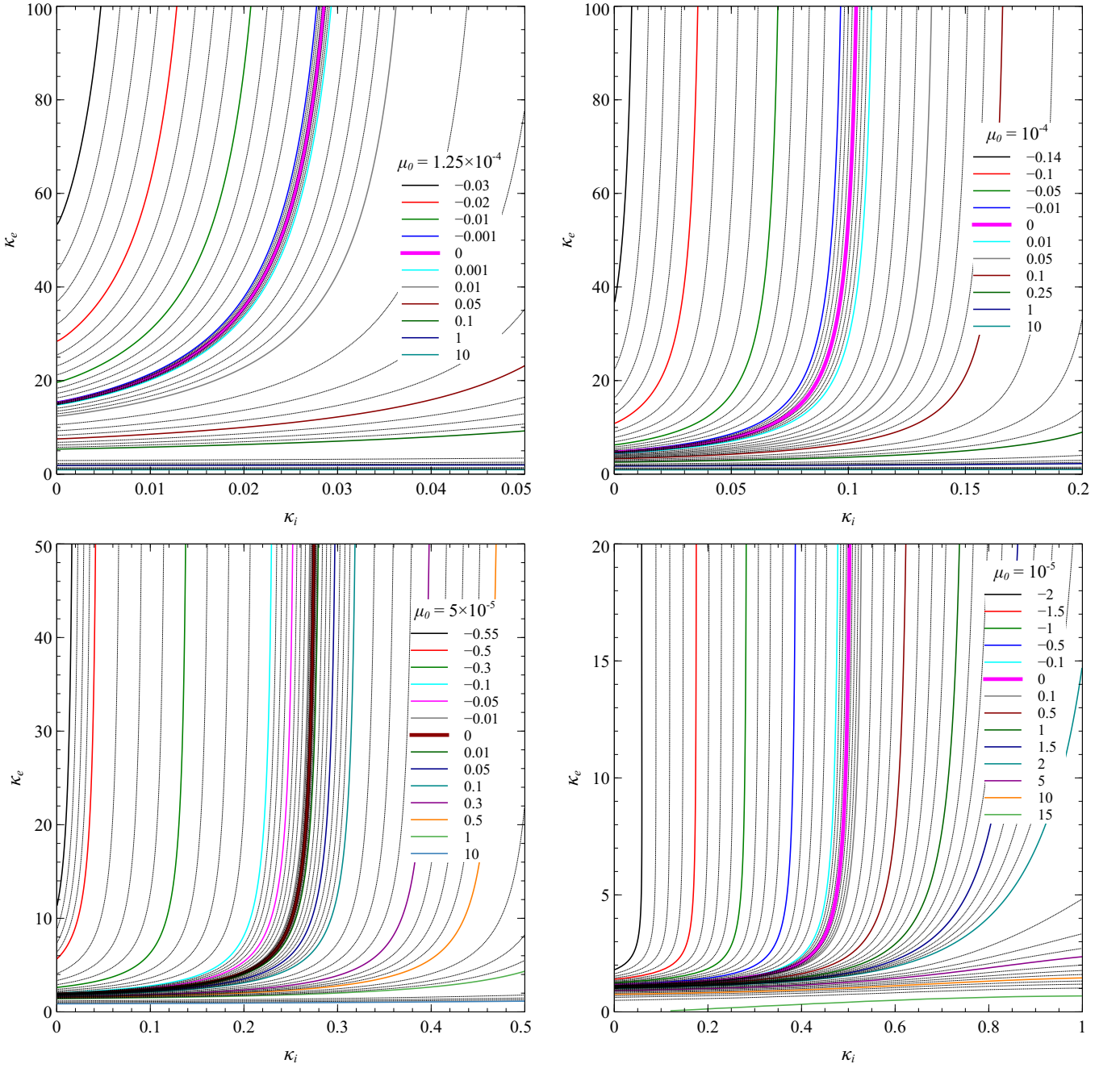


Figure 4. Contour plots of the normalized potential  $\chi_e = Z_d / \tau_e \tilde{a}$  as function of  $\kappa_e \times \kappa_i$  for several values of  $\mu_{e0} = \mu_{i0} = \mu_0$ .

## B. Model 2

Model 2, which was discussed in section IV C, is a model in which the kinetic temperature is  $\kappa$ -invariant and thus serve as a measure of a physical temperature. Some results of the equilibrium electric charge that a dust grain acquires due to collisions of suprathermal plasma particles described by model 2 are presented here. The results will be presented again with the combinations of distributions comprised by the cases 1 – 4 described at

the beginning of the section.

Figure 5 shows plots of the dust charge number for cases 1 and 2. The charge numbers were obtained from the solutions of (9), employing the collision factors (12a, b) and (11a, b).

The left panel of Fig. 5 shows the ratio  $Z_d^{(\text{case 1})} / Z_d^{(\text{M})}$  as a function of  $\kappa_e$  for several values of  $\mu_{e0}$ . The results obtained from model 2 differ significantly from model 1, which were shown by Fig. 1. Now, instead of a steady increase of the charge ratio with diminishing  $\kappa_e$ , we ob-

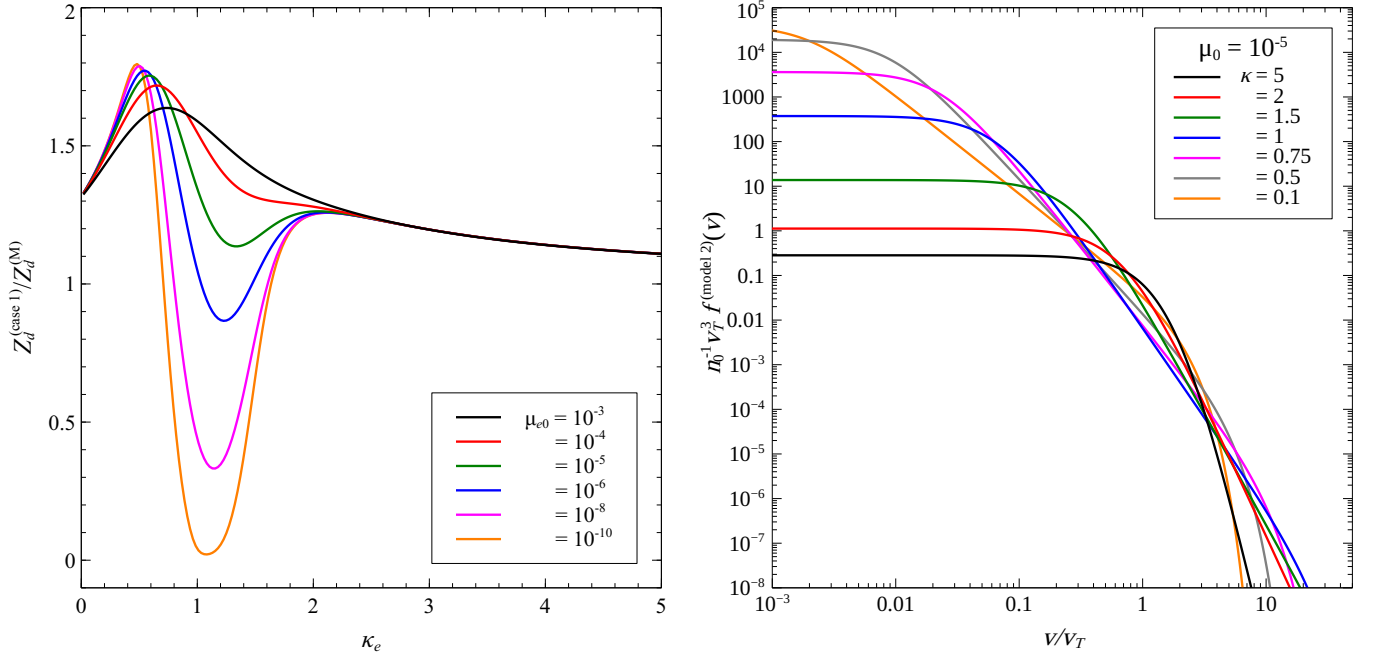


Figure 5. (Left panel) Plots of  $Z_d^{(\text{case 1})}/Z_d^{(M)}$  as solutions of eq. (9) for model 2, case 1 as functions of  $\kappa_e$ . (Right panel) log-log plots of the normalized RKD for fixed  $\mu_0$  and several values of  $\kappa$ .

serve initially a slight increase until  $\kappa_e \approx 2$  that is independent on  $\mu_{e0}$ . Then, for  $\kappa_e \lesssim 2$  the ratio curves split for different regularization parameters. For the larger value ( $\mu_{e0} = 10^{-3}$ ), the ratio continues to grow until  $\kappa_e \approx 0.75$  and then it drops to the limiting value of  $Z_d^{(\text{case 1})} \approx 1.32Z_d^{(M)}$  at  $\kappa_e = 0$ . However, the results for  $\mu_{e0} \leq 10^{-5}$  present a more complex behavior. All these plots display a region of diminishing charge ratio, with minima located in the region  $1 < \kappa_e < 1.4$  that are smaller for smaller  $\mu_{e0}$ , and then the ratio eventually starts to grow and diminish again as  $\kappa_e$  keeps on reducing, until eventually converging all to the same limiting value at  $\kappa_e = 0$ .

The behavior of the dust charge displayed by the left panel of Fig. 5 hints at the possibility of positively-charged grains when the regularization parameter for the electronic VDF is sufficiently small, occurring at low (but not too low) values of the kappa index. Notice that this could occur even when the ions are thermal, which is the case here. Moreover, although  $\kappa_e \sim 1$  is not too low, it is close to limit of validity of standard Kappa distributions, which is where the difference between RKDs and SKDs is the greatest and is the reason why this behavior was not observed before. It is the regularization action carried out by the parameter  $\mu_0$  that allows the existence of plasmas with a higher state of suprathermality.

The stark difference between the behavior observed with model 2 in comparison with model 1 is due to the fact that in order to maintain the kinetic temperature invariant when varying  $\kappa$ , both the core and the tail of the VDF must be modified. The right panel of Fig. 5 shows

log-log plots of the model-2 VDF versus speed for fixed  $\mu_{e0} = 10^{-5}$  and several values of  $\kappa$ . Looking separately the core and the tail portions of the VDF, one notices that the core region steadily grows with diminishing  $\kappa_e$ , but remains relatively constant (in the log scale) up to  $v \lesssim v_T$ . However, for very low kappa-index ( $\kappa_e = 0.1$ ) the probability level quickly reduces with speed. Looking now at the tail, one notices that for  $\kappa_e > 1$  (at values permissible for SKDs), the population level of the tail increases with speed, at least within the mid-energy range displayed ( $v/v_T < 50$ ). However for higher energy, the action of the regularization parameter kicks in earlier. This is noticeable in the plots for  $\kappa_e < 1$ , where one already notices a reduction in the population level at the tail that is more pronounced for smaller  $\kappa_e$ . Hence, a model-2 RKD keeps the kinetic temperature  $\kappa$ -invariant by “removing” particles from the tail and “injecting” them in the core. Therefore, the results of the left panel of Fig. 5 can be explained by the fact that for small  $\kappa_e$  there are in fact less high-energy electrons that can successfully collide and become attached to the grain, thereby reducing the net negative charge.

Figure 6 displays some results for case 2. Once again, the solutions are displayed as charge number ratio versus  $\kappa_i$  and the results can be compared with Fig. 2. One observes again the splitting of the curves with  $\mu_{i0}$  for  $\kappa_i \lesssim 2$  and the possibility of charge inversion for very small values of the regularization parameter. The depleted portions at  $\kappa_i \lesssim 1$  can be understood in terms of the previous interpretation and by the fact that an excess of slower ions increases the collisional cross-section

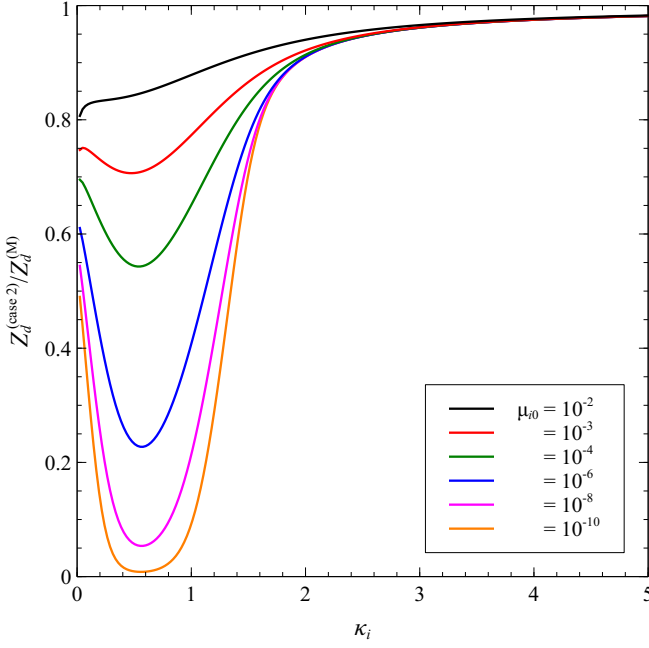


Figure 6. Plots of  $Z_d^{(\text{case 2})}/Z_d^{(M)}$  as solutions of eq. (9) for model 2, case 2 as functions of  $\kappa_i$ .

contained in the integration of the collision frequency (1).

Investigation of the null-charge condition from model 2 also leads to very different conclusions, as compared with model 1. Now, the condition  $\chi_e = 0$  is met when the set  $\{\mu_{e0}, \kappa_e, \mu_{i0}, \kappa_i\}$  satisfies

$$\begin{aligned} \sqrt{\phi_i}^{[1]} \mathcal{U}(\kappa_i, \kappa_i + 1, \mu_i) \\ = \sqrt{\frac{m_i}{m_e} \tau_e \phi_e}^{[1]} \mathcal{U}(\kappa_e, \kappa_e + 1, \mu_e), \end{aligned} \quad (14)$$

with  $\phi_\beta = \mathcal{U}^{[2]}(\kappa_\beta, \kappa_\beta + 1, \mu_\beta)$ .

Figure 7 shows some solutions of (14). One obvious difference from Fig. 3 is that the values of the kappa indices are within the same order of magnitude, whereas the regularization parameters are quite different.

Starting with the black curves, corresponding to a very small  $\mu_{e0} = 10^{-12}$  and a relatively large  $\mu_{i0} = 10^{-1}$ , we observe that there are two curves in the  $\kappa_e \times \kappa_i$  plane where the condition  $\chi_e = 0$  is satisfied. Grains with positive charge (*i.e.*, with  $\chi_e < 0$ ) occur in the region within the curves. Keeping  $\mu_{e0}$  fixed and reducing  $\mu_{i0}$ , we observe that both curves converge to the point  $\kappa_e \approx \kappa_i \approx 1$ , which eventually becomes an X point, where both curves coalesce and split, leaving a region (for  $\mu_{i0} < 2.5 \times 10^{-3}$ ) with no solution. As  $\mu_{i0}$  keeps on diminishing, this region enlarges. Hence, the null-charge condition becomes harder to be satisfied as  $\mu_{i0}$  approaches  $\mu_{e0}$  from above.

Reducing the fixed value to  $\mu_{e0} = 10^{-14}$  and repeating the steps with  $\mu_{i0} = 10^{-1}$  downwards, we observe the same process, with the difference that the distance

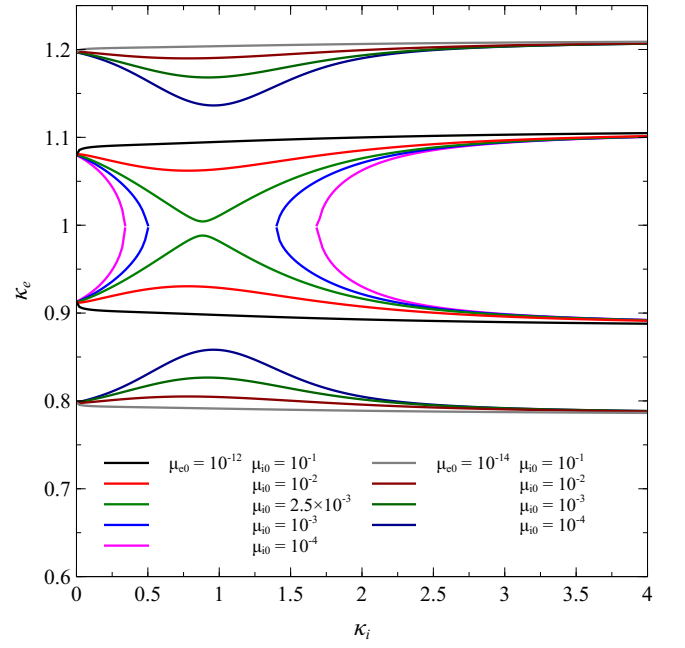


Figure 7. Plots of  $\kappa_e$  and  $\kappa_i$  values as solutions of the null-charge condition (14), for different values of the set  $\{\mu_{e0}, \kappa_e, \mu_{i0}, \kappa_i\}$ .

between the initial curves widened. Conversely, if we increase the value of  $\mu_{e0}$ , the distance shrinks, until, eventually, for  $\mu_{e0} \gtrsim 5 \times 10^{-12}$  the condition  $\chi_e = 0$  is no longer satisfied for any  $\mu_{i0}$ .

Therefore, the conditions for positively-charged dust when the plasma is described by model-2 regularized distributions, are very different from the conditions for model 1. Now, in order for the grains to become positive, the kappa-indices of both electrons and ions can be of the same order, but the regularization parameters must be very different, with  $\mu_{e0} \ll \mu_{i0}$ .

As a final display of results for model 2, figure 8 shows contour plots of the normalized potential  $\chi_e$  as a function of  $\kappa_e \times \kappa_i$  for the first set of parameters of Fig. 7,  $\mu_{e0} = 10^{-12}$  and  $\mu_{i0} = 10^{-1}$ . One can clearly observe the disjoint contours marking the null-charge condition ( $\chi_e = 0$ ), with positively-charged grains occurring within the delimited region and negatively-charged grains without. The largest negative potential that occurs within the black contour ( $\chi_{e,\min} = -1.67 \times 10^{-5}$ ) is very small compared with the nominal Maxwellian value.

As a summary, results from model 2 also show that in the majority of situations the dust charge is negative, but it can be positive under very restrictive conditions, which are quite different from the conditions imposed by model 1. Now, the electronic and ionic kappa-indices can be of the same order of magnitude, but the regularization parameters must be vastly different, with  $\mu_{e0} \ll \mu_{i0}$ . This particular scenario happens due to the specific characteristic attributed to model 2, namely, that the kinetic temperature must remain invariant to the kappa-index.



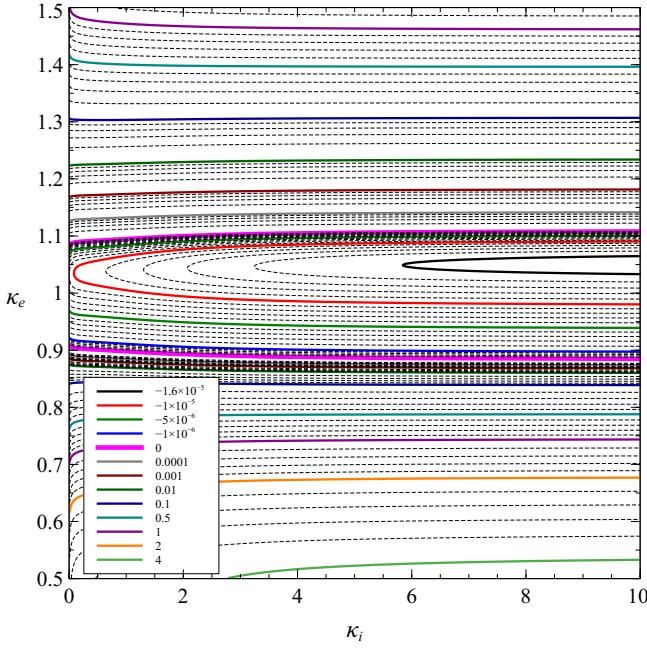


Figure 8. Contour plots of the normalized potential  $\chi_e = Z_d / \tau_e \tilde{a}$  as a function of  $\kappa_e \times \kappa_i$  for model 2, with fixed  $\mu_{e0} = 10^{-12}$  and  $\mu_{i0} = 10^{-1}$ .

As we have concluded with model 1, such disparity of suprathermal states between the plasma species makes it highly unlikely that such situation will ever be found in naturally-occurring environments.

## VI. FINAL REMARKS

In this work we have discussed the charging of spherical dust grains immersed in an infinite, homogeneous, and steady-state plasma, composed by electrons and one positive ion species, when the velocity distribution functions of both species are the  $\kappa$ -regularized distribution. Differently from the Kappa distributions considered in Paper I, the RKD can describe states of extreme suprathermality, which are achieved when  $\kappa + \alpha \leq 3/2$  (with any  $\kappa > 0$ ), thanks to the presence of a Gaussian factor, determined by the regularization parameter  $\mu \ll 1$ . The RKD reduces to the standard Kappa distribution when  $\mu = 0$  (in which case it is only valid when  $\kappa + \alpha > 3/2$ ) and to the Maxwellian when  $\kappa \rightarrow \infty$ .

From a generalized expression for the RKD, we have considered two common models, frequently employed in the literature. Model 1 assumes a free parameter  $\theta = \sqrt{2T/m}$ , for which the quantity  $T$  is not the physical temperature of the system (*i.e.*, is not the kinetic temperature, nor is derived from an entropic principle), and Model 2, for which the kinetic temperature is  $\kappa$ -invariant and can be derived from an entropy formulation.

The equation that determines the equilibrium charge of the dust grains due to inelastic collisions with the

plasma particles was solved for both models with different combinations of velocity distribution functions: one case, where the electrons are suprathermal and the ions are Maxwellian. Another case, where the ions are suprathermal while the electrons are thermal, and final cases where both species are suprathermal. The solutions were mostly sought in the small-kappa range, which is where the distinction between the effects from regularized Kappa distributions, as compared to standard Kappa distributions, is more pronounced.

When solving the equation employing model 1 for the first case, it was observed that the grains still acquire a net negative charge, but with higher absolute value, as it was already observed in Paper I, where standard Kappa distributions were employed. This happens due to the excess of high-energy electrons when the species is in a suprathermal state. For small  $\kappa_e \lesssim 1$ , the negative charge eventually saturates.

Contrastingly, in the second case (suprathermal ions, thermal electrons) the dust charge reduces with  $\kappa_i$ , reaching a minimum value at  $\kappa_i = 0$  that depends on the regularization parameter  $\mu_i$ . For sufficiently small values of  $\{\mu_{i0}, \kappa_i\}$ , the dust can become positively-charged due to the extreme suprathermality of the ions as compared to electrons. This result can be obtained even when the electrons are suprathermal. After investigating in further details this possibility, it was concluded that indeed the dust can become positively-charged due to collisions alone, a result that is impossible in a thermal plasma, but only when the ions are much more suprathermal than the electrons, meaning that  $\kappa_i \ll \kappa_e$  is a necessary condition.

When investigating the possibility of positive charge of grains immersed in plasmas described by model 2, it was observed that this can happen when  $\kappa_i$  and  $\kappa_e$  are of the same order of magnitude, but only when the regularization parameters are vastly different, with  $\mu_{e0} \ll \mu_{i0}$ . This happens due to the requirement of the model 2 that the kinetic temperature is independent on the kappa index. As  $\kappa$  reduces, the core region of the VDF becomes more populated whereas the high-energy tail becomes depleted. Consequently, the grain can become positively-charged because there are fewer high-energy electrons to overcome a negative potential and more low-energy ions with higher cross section. In this case, a balance can be achieved where the number of positive ions attaching to the grain's surface overcomes the number of negative electrons. This is a different situation where the ions are more suprathermal than electrons, with the suprathermality states determined mostly by the regularization parameters, instead of the kappa indices.

This work considered only the collisional charging of the dust grains. More complete treatments, to appear in future publications, will include other relevant charging mechanisms such as photoelectric and secondary emissions. Future work will also investigate the effect of charged dust in suprathermal plasma in wave propagation and wave-particle interactions.

In this Paper, we applied the formalism to a dusty

plasma environment typical of carbon-rich stars. Future applications will consider different plasma conditions found in other space and astrophysical systems.

This line of investigation can also be extended to other plasma phenomena, such as magnetic reconnection. There is evidence that the disruption of the current sheet equilibrium of opposing magnetic flux tubes is closely related to magnetic reconnection and the level of turbulence inferred at the top of coronal mass ejections.<sup>99</sup> On one hand, theoretical studies of the effect of electronic depletion on the Harris current sheet and other nonlinear structures can lead to slower reconnection rates on dusty plasmas.<sup>100,101</sup> On the other hand, the presence of extreme suprathermal particles described by the regularized distributions allows the formation of modified Harris sheets characterized by higher values of plasma parameters such as density, current, magnetic field and temperature, which can, contrastingly, result in higher reconnection rates.<sup>84</sup> Hence, further studies that combine both extensions to the traditional treatment of magnetic reconnection, the presence of dust grains and extreme suprathermal particles, could provide interesting contributions to this important phenomenon observed in various astrophysical systems.

## ACKNOWLEDGMENTS

RG acknowledges support provided by Conselho Nacional de Desenvolvimento Científico e Tecnológico (CNPq, Brazil), Grant No. 313330/2021-2. LFZ acknowledges support from CNPq, grant No. 303189/2022-3. This study was financed in part by Coordenação de Aperfeiçoamento de Pessoal de Nível Superior (CAPES, Brazil) - Finance Code 001.

## DATA AVAILABILITY

The data that support the findings of this study are available from the corresponding author upon reasonable request.

## Appendix A: Properties and limiting cases of the function ${}^{[m]}\mathcal{W}^{[n]}(\eta, \zeta, \mu)$

The function  ${}^{[m]}\mathcal{W}^{[n]}(\eta, \zeta, \mu)$  is defined by (6a). The expression employed in this work differs from the original definition from Ref. 78 because we are considering cases where  $\zeta \geq 0$  always.

One trivial limiting case occurs when  $n = m$ ,

$${}^{[m]}\mathcal{W}^{[m]}(\eta, \zeta, \mu) = 1.$$

Another obvious property is the permutation of indices  $m \leftrightarrow n$ , which leads to

$${}^{[n]}\mathcal{W}^{[m]}(\eta, \zeta, \mu) = \left[ {}^{[m]}\mathcal{W}^{[n]}(\eta, \zeta, \mu) \right]^{-1}. \quad (\text{A1})$$

Yet another obvious property is

$${}^{[m]}\mathcal{W}^{[\ell]}(\eta, \zeta, \mu) {}^{[\ell]}\mathcal{W}^{[n]}(\eta, \zeta, \mu) = {}^{[m]}\mathcal{W}^{[n]}(\eta, \zeta, \mu).$$

Other important identities involving the Tricomi function are given below.<sup>80</sup> Firstly, the integral representation

$$U(a, b, z) = \frac{1}{\Gamma(a)} \int_0^\infty dt t^{a-1} (1+t)^{b-a-1} e^{-zt}, \quad (\text{A2})$$

which is valid for  $\Re a > 0$  and  $|\arg(z)| < \pi/2$ . And the Kummer transformation

$$U(a, b, z) = z^{1-b} U(a-b+1, 2-b, z). \quad (\text{A3})$$

Important cases in the analysis performed in this paper involve the possible limits of vanishing argument of the Tricomi functions in (6a). The limit  $\kappa\mu(\kappa) \rightarrow 0$  involves both limits  $\kappa \rightarrow 0$  and  $\kappa \rightarrow \infty$ . These limits are obtained from the general limiting cases given by Ref. 80, sec. 13.2(iii). Given the Tricomi function  $U(a, b, z)$ , the limiting cases for  $z \rightarrow 0$  in the aforementioned reference consider a total of 7 different possible ranges of values of the parameter  $b$ . Since the function  ${}^{[m]}\mathcal{W}^{[n]}(\eta, \zeta, \mu)$  depends on the double set of indices  $\{m, n\}$ , it means that a total of 49 cases for  $\zeta$  must be considered.

A straightforward but rather tedious analysis of all possible cases leads to the following limits. If  $\zeta = \frac{3+m}{2}$  and  $\zeta > \frac{3+n}{2}$ , or  $\zeta > \frac{3+m}{2}$  and  $\zeta = \frac{3+n}{2}$ ,

$$\lim_{\mu\eta \rightarrow 0} {}^{[m]}\mathcal{W}^{[n]}(\eta, \zeta, \mu) = \frac{\Gamma(\zeta - \frac{3+m}{2})}{\Gamma(\zeta - \frac{3+n}{2})}.$$

The remaining cases, which occur when either  $\zeta < \frac{3+m}{2}$  or  $\zeta < \frac{3+n}{2}$ , are not reproducible by the formula above and are

$$\lim_{\mu\eta \rightarrow 0} {}^{[m]}\mathcal{W}^{[n]}(\eta, \zeta, \mu) \rightarrow \begin{cases} 0, & n > m \\ \infty, & n < m. \end{cases}$$

## REFERENCES

- <sup>1</sup>C. K. Goertz, *Rev. Geophys.* **27**, 271–292 (1989).
- <sup>2</sup>T. G. Northrop, *Phys. Scripta* **45**, 475 (1992).
- <sup>3</sup>D. A. Mendis and M. Rosenberg, *Annu. Rev. Astron. Astrophys.* **32**, 419–463 (1994).
- <sup>4</sup>P. K. Shukla and A. A. Mamun, *Introduction to Dusty Plasma Physics*, edited by A. A. Mamun, Series in Plasma Physics (Taylor & Francis, Inc., New York, 2002) p. 450.
- <sup>5</sup>V. N. Tsytovich, G. E. Morfill, and H. Thomas, *Plasma Phys. Rep.* **30**, 816–864 (2004).
- <sup>6</sup>V. E. Fortov, A. V. Ivlev, S. A. Khrapak, A. G. Khrapak, and G. E. Morfill, *Physics Reports* **421**, 1–103 (2005).
- <sup>7</sup>I. Mann, A. Czechowski, N. Meyer-Vernet, A. Zaslavsky, and H. Lamy, *Plasma Phys. Cont. Fusion* **52**, 124012 (2010).
- <sup>8</sup>I. Mann, N. Meyer-Vernet, and A. Czechowski, *Phys. Rep.* **536**, 1–39 (2014).
- <sup>9</sup>F. Spahn, M. Sachse, M. Seiß, H.-W. Hsu, S. Kempf, and M. Horányi, *Space Sci. Rev.* **215**, 11 (2019).
- <sup>10</sup>A. Melzer, H. Krüger, D. Maier, and S. Schütt, *Rev. Mod. Plasma Phys.* **5**, 11 (2021).

- <sup>11</sup>V. J. Sterken, L. R. Baalmann, B. T. Draine, E. Godenko, K. Herbst, H.-W. Hsu, S. Hunziker, V. Izmodenov, R. Lalletment, and J. D. Slavin, *Space Sci. Rev.* **218**, 71 (2022).
- <sup>12</sup>E. Godenko and V. Izmodenov, *Adv. Space Res.* **72**, 5142–5158 (2023).
- <sup>13</sup>E. P. Lieb, R. M. Lau, J. L. Hoffman, M. F. Corcoran, M. Garcia Marin, T. R. Gull, K. Hamaguchi, Y. Han, M. J. Hankins, O. C. Jones, T. I. Madura, S. V. Marchenko, H. Matsuhara, F. Millour, A. F. J. Moffat, M. R. Morris, P. W. Morris, T. Onaka, M. D. Perrin, A. Rest, N. Richardson, C. M. P. Russell, J. Sanchez-Bermudez, A. Soulain, P. Tuthill, G. Weigelt, and P. M. Williams, *Astrophys. J. Lett.* **979**, L3 (2025).
- <sup>14</sup>H. Kimura and I. Mann, *Astrophys. J.* **499**, 454–462 (1998).
- <sup>15</sup>A. M. Ignatov, *Plasma Phys. Rep.* **35**, 647–650 (2009).
- <sup>16</sup>R. A. Galvão and L. F. Ziebell, *Phys. Plasmas* **19**, 093702 (2012).
- <sup>17</sup>J. C. Ibáñez-Mejía, S. Walch, A. V. Ivlev, S. Clarke, P. Caselli, and P. R. Joshi, *Mont. Not. R. Astron. Soc.* **485**, 1220–1247 (2019).
- <sup>18</sup>S. K. Kodanova, N. K. Bastykova, T. S. Ramazanov, G. N. Nigmatova, S. A. Maiorov, and Z. A. Moldabekov, *IEEE Trans. Plasma Sci.* **47**, 3052–3056 (2019).
- <sup>19</sup>R. U. Masheyeva, K. N. Dzhumagulova, and M. Myrzaly, *Plasma Phys. Rep.* **48**, 1203–1210 (2022).
- <sup>20</sup>N. D’Angelo, *Planet. Space Sci.* **38**, 1143–1146 (1990).
- <sup>21</sup>M. R. Amin, *Phys. Rev. E* **54**, R2232–R2235 (1996).
- <sup>22</sup>T. K. Baluku and M. A. Hellberg, *Phys. Plasmas* **22**, 083701 (2015), 10.1063/1.4927581.
- <sup>23</sup>S. Bhakta, U. Ghosh, and S. Sarkar, *Phys. Plasmas* **24**, 023704 (2017).
- <sup>24</sup>A. I. Momot, A. G. Zagorodny, and O. V. Momot, *Phys. Plasmas* **25**, 073706 (2018).
- <sup>25</sup>M. C. de Juli and R. S. Schneider, *J. Plasma Phys.* **60**, 243–263 (1998).
- <sup>26</sup>D. Falceta-Gonçalves and V. Jatenco-Pereira, *Astrophys. J.* **576**, 976–981 (2002).
- <sup>27</sup>M. C. de Juli, R. S. Schneider, L. F. Ziebell, and V. Jatenco-Pereira, *Phys. Plasmas* **12**, 052109 (2005).
- <sup>28</sup>A. A. Vidotto and V. Jatenco-Pereira, *Astrophys. J.* **639**, 416–422 (2006).
- <sup>29</sup>M. C. de Juli, R. S. Schneider, L. F. Ziebell, and R. Gaelzer, *Phys. Plasmas* **14**, 022104 (2007).
- <sup>30</sup>M. C. de Juli, R. S. Schneider, L. F. Ziebell, and R. Gaelzer, *J. Geophys. Res.* **112**, A10105 (2007).
- <sup>31</sup>R. Gaelzer, M. C. de Juli, R. S. Schneider, and L. F. Ziebell, *Plasma Phys. Cont. Fusion* **51**, 015011 (17pp) (2009).
- <sup>32</sup>M. C. de Juli, R. S. Schneider, L. F. Ziebell, and R. Gaelzer, *Braz. J. Phys.* **39**, 111–132 (2009).
- <sup>33</sup>V. Jatenco-Pereira, A. C.-L. Chian, and N. Rubab, *Nonl. Proc. Geophys.* **21**, 405–416 (2014).
- <sup>34</sup>L. B. De Toni and R. Gaelzer, *Mont. Not. R. Astron. Soc.* **508**, 340–351 (2021).
- <sup>35</sup>L. B. De Toni, R. Gaelzer, and L. F. Ziebell, *Mont. Not. R. Astron. Soc.* **516**, 4650–4659 (2022).
- <sup>36</sup>L. B. De Toni, R. Gaelzer, and L. F. Ziebell, *Mont. Not. R. Astron. Soc.* **512**, 1795–1804 (2022).
- <sup>37</sup>L. B. De Toni, R. Gaelzer, and L. F. Ziebell, *Mont. Not. R. Astron. Soc.* **529**, 3003–3012 (2024).
- <sup>38</sup>R. A. Treumann, C. H. Jaroschek, and M. Scholer, *Phys. Plasmas* **11**, 1317–1325 (2004).
- <sup>39</sup>M. L. Goldstein, R. T. Wicks, S. Perri, and F. Sahraoui, *Phil. Trans. R. Soc. A* **373** (2015), 10.1098/rsta.2014.0147.
- <sup>40</sup>Howes G. G., *Phil. Trans. R. Soc. A* **373** (2015), 10.1098/rsta.2014.0145.
- <sup>41</sup>K. Ferrière, *Plasma Phys. Cont. Fusion* **62**, 014014 (2020).
- <sup>42</sup>F. Sahraoui, L. Hadid, and S. Huang, *Rev. Mod. Plasma Phys.* **4**, 4 (2020).
- <sup>43</sup>G. Livadiotis, *Kappa Distributions: Theory and Applications in Plasmas* (Elsevier Science & Technology Books, 2017).
- <sup>44</sup>M. Lazar and H. Fichtner, eds., *Kappa Distributions: From Observational Evidences via Controversial Predictions to a Consistent Theory of Nonequilibrium Plasmas*, Astrophysics and Space Science Library, Vol. 464 (Springer, Cham, 2021).
- <sup>45</sup>R. Gaelzer, M. C. de Juli, and L. F. Ziebell, *J. Geophys. Res.* **115** (2010), 10.1029/2009JA015217.
- <sup>46</sup>N. Rubab, N. V. Erkaev, D. Langmayr, and H. K. Biernat, *Phys. Plasmas* **17**, 103704 (2010).
- <sup>47</sup>F. Deeba, Z. Ahmad, and G. Murtaza, *Phys. Plasmas* **18**, 072104 (2011).
- <sup>48</sup>R. Galvão, L. F. Ziebell, R. Gaelzer, and M. C. de Juli, *Braz. J. Phys.* **41**, 258–274 (2011).
- <sup>49</sup>R. A. Galvão, L. F. Ziebell, R. Gaelzer, and M. C. de Juli, *Phys. Plasmas* **19**, 123705 (2012), 10.1063/1.4772771.
- <sup>50</sup>M. Shahmansouri and M. Tribeche, *Astrophys. Space Sci.* **342**, 87–92 (2012).
- <sup>51</sup>M. S. dos Santos, L. F. Ziebell, and R. Gaelzer, *Phys. Plasmas* **23**, 013705 (2016), 10.1063/1.4939885.
- <sup>52</sup>M. S. dos Santos, L. F. Ziebell, and R. Gaelzer, *Astrophys. Space Sci.* **362**, 18 (2017).
- <sup>53</sup>L. F. Ziebell, R. Gaelzer, and F. J. R. Simões, *J. Plasma Phys.* **83** (2017), 10.1017/S0022377817000733.
- <sup>54</sup>L. F. Ziebell and R. Gaelzer, “Collisional charging of dust particles by suprathermal particles. I – Standard anisotropic Kappa distributions,” (2024), submitted for publication.
- <sup>55</sup>I. Mann, A. Pellinen-Wannberg, E. Murad, O. Popova, N. Meyer-Vernet, M. Rosenberg, T. Mukai, A. Czechowski, S. Mukai, J. Safrankova, and Z. Nemecek, *Space Sci. Rev.* **161**, 1–47 (2011).
- <sup>56</sup>S. Misra and S. K. Mishra, *Mont. Not. R. Astron. Soc.* **432**, 2985–2993 (2013).
- <sup>57</sup>Q. Ma, L. S. Matthews, V. Land, and T. W. Hyde, *Astrophys. J.* **763**, 77 (2013).
- <sup>58</sup>J. E. Allen, *Phys. Scripta* **45**, 497 (1992).
- <sup>59</sup>A. Melzer, *Physics of Dusty Plasmas: An Introduction*, Lecture Notes in Physics (Springer Cham, 2019) 235 + x pp.
- <sup>60</sup>M. Salimullah, I. Sandberg, and P. K. Shukla, *Phys. Rev. E* **68**, 027403 (2003).
- <sup>61</sup>J. S. Chang and K. Spariosu, *J. Phys. Soc. Jpn.* **62**, 97–104 (1993).
- <sup>62</sup>H. Davari, B. Farokhi, and M. Ali Asgarian, *Sci. Rep.* **13**, 1111 (2023).
- <sup>63</sup>V. M. Vasyliunas, *J. Geophys. Res.* **73**, 2839–2884 (1968).
- <sup>64</sup>M. A. Hellberg, R. L. Mace, T. K. Baluku, I. Kourakis, and N. S. Saini, *Phys. Plasmas* **16**, 094701 (2009).
- <sup>65</sup>L.-N. Hau, W.-Z. Fu, and S.-H. Chuang, *Phys. Plasmas* **16**, 094702 (2009).
- <sup>66</sup>K. Scherer, H. Fichtner, and M. Lazar, *Europhys. Lett.* **120**, 50002 (2017).
- <sup>67</sup>H. Fichtner, K. Scherer, M. Lazar, H. J. Fahr, and Z. Vörös, *Phys. Rev. E* **98**, 053205 (2018).
- <sup>68</sup>R. Gaelzer and L. F. Ziebell, *J. Geophys. Res.* **119**, 9334–9356 (2014).
- <sup>69</sup>R. Gaelzer and L. F. Ziebell, *Phys. Plasmas* **23**, 022110 (2016).
- <sup>70</sup>R. A. Askey and R. Roy, in *NIST Handbook of Mathematical Functions*, edited by F. W. J. Olver, D. W. Lozier, R. F. Boisvert, and C. W. Clark (Cambridge, New York, 2010) Chap. 5, p. 135–147.
- <sup>71</sup>R. Gaelzer, L. F. Ziebell, and A. R. Meneses, *Phys. Plasmas* **23**, 062108 (2016).
- <sup>72</sup>M. Maksimovic, I. Zouganelis, J. Y. Chaufray, K. Issautier, E. E. Scime, J. E. Littleton, E. Marsch, D. J. McComas, C. Salem, R. P. Lin, and H. Elliot, *J. Geophys. Res.* **110**, A09104 (2005).
- <sup>73</sup>S. Štverák, P. Trávníček, M. Maksimovic, E. Marsch, A. N. Fazakerley, and E. E. Scime, *J. Geophys. Res.* **113**, A03103 (2008).
- <sup>74</sup>S. Štverák, M. Maksimovic, P. M. Trávníček, E. Marsch, A. N. Fazakerley, and E. E. Scime, *J. Geophys. Res.* **114**, A05104 (2009).
- <sup>75</sup>L. B. Wilson III, L.-J. Chen, S. Wang, S. J. Schwartz, D. L. Turner, M. L. Stevens, J. C. Kasper, A. Osmane, D. Caprioli,

- S. D. Bale, M. P. Pulupa, C. S. Salem, and K. A. Goodrich, *apjss* **243**, 8 (2019).
- <sup>76</sup>L. B. Wilson III, K. A. Goodrich, D. L. Turner, I. J. Cohen, P. L. Whittlesey, and S. J. Schwartz, *Front. Astron. Space Sci.* **9** (2022), 10.3389/fspas.2022.1063841.
- <sup>77</sup>G. Livadiotis, D. J. McComas, H. O. Funsten, N. A. Schwadron, J. R. Szalay, and E. Zirnstien, *Astrophys. J. Suppl. Ser.* **262**, 53 (2022).
- <sup>78</sup>K. Scherer, E. Husidic, M. Lazar, and H. Fichtner, *Mont. Not. R. Astron. Soc.* **497**, 1738–1756 (2020).
- <sup>79</sup>R. Gaelzer, H. Fichtner, and K. Scherer, *Phys. Plasmas* **31**, 072112 (2024).
- <sup>80</sup>A. B. O. Daalhuis, in *NIST Handbook of Mathematical Functions*, edited by F. W. J. Olver, D. W. Lozier, R. F. Boisvert, and C. W. Clark (Cambridge, New York, 2010) Chap. 13, p. 321–349.
- <sup>81</sup>E. Husidic, K. Scherer, M. Lazar, H. Fichtner, and S. Poedts, *Astrophys. J.* **927**, 159 (2022).
- <sup>82</sup>K. Scherer, E. Husidic, M. Lazar, and H. Fichtner, *Astron. Astrophys.* **663**, A67 (2022).
- <sup>83</sup>V. Pierrard, M. Péters de Bonhome, J. Halekas, C. Audoor, P. Whittlesey, and R. Livi, *Plasma* **6**, 518–540 (2023).
- <sup>84</sup>L.-N. Hau, C.-K. Chang, and M. Lazar, *Astrophys. J.* **956**, 144 (2023).
- <sup>85</sup>Y. Liu, *Braz. J. Phys.* **54**, 5 (2024).
- <sup>86</sup>P. H. Yoon, M. Lazar, K. Scherer, H. Fichtner, and R. Schlickeiser, *Astrophys. J.* **868**, 131 (2018).
- <sup>87</sup>P. H. Yoon, “Non-equilibrium Statistical Mechanics of Electron Kappa Distribution,” p. 235–277, vol. 464 of <sup>44</sup> (2021).
- <sup>88</sup>G. Livadiotis and D. J. McComas, *J. Geophys. Res.* **114**, A11105 (2009).
- <sup>89</sup>G. Livadiotis and D. J. McComas, *Entropy* **23**, 1683 (2021).
- <sup>90</sup>G. Livadiotis and D. J. McComas, *Astrophys. J.* **940**, 83 (2022).
- <sup>91</sup>G. Livadiotis and D. J. McComas, *Europhys. Lett.* **146**, 41003 (2024).
- <sup>92</sup>M. P. Leubner, *Astrophys. Space Sci.* **282**, 573–579 (2002).
- <sup>93</sup>Lazar, M., Pierrard, V., Shaaban, S. M., Fichtner, H., and Poedts, S., *Astron. Astrophys.* **602**, A44 (2017).
- <sup>94</sup>A. V. Eyelade, M. Stepanova, C. M. Espinoza, and P. S. Moya, *Astrophys. J. Suppl. Ser.* **253**, 34 (2021).
- <sup>95</sup>I. P. Kirpichev, E. E. Antonova, M. Stepanova, A. V. Eyelade, C. M. Espinoza, I. L. Ovchinnikov, V. G. Vorobjev, and O. I. Yagodkina, *J. Geophys. Res.* **126**, e2021JA029409 (2021).
- <sup>96</sup>X. Zheng, M. M. Martinović, V. Pierrard, K. G. Klein, M. Liu, J. B. Abraham, Y. Liu, J. Luo, X. Lin, G. Liu, and J. Li, *Astrophys. J.* **977**, 39 (2024).
- <sup>97</sup>G. Livadiotis, M. I. Desai, and L. B. Wilson, III, *Astrophys. J.* **853**, 142 (2018).
- <sup>98</sup>M. E. Cuesta, A. T. Cummings, G. Livadiotis, D. J. McComas, C. M. S. Cohen, L. Y. Khoo, T. Sharma, M. M. Shen, R. Bandyopadhyay, J. S. Rankin, J. R. Szalay, H. A. Farooki, Z. Xu, G. D. Muro, M. L. Stevens, and S. D. Bale, *Astrophys. J.* **973**, 76 (2024).
- <sup>99</sup>A. C.-L. Chian, H. Q. Feng, Q. Hu, M. H. Loew, R. A. Miranda, P. R. Muñoz, D. G. Sibeck, and D. J. Wu, *Astrophys. J.* **832**, 179 (2016).
- <sup>100</sup>S. A. Lazerson, *J. Plasma Phys.* **77**, 31–37 (2011).
- <sup>101</sup>S.-D. Yang, L. Wang, and C. Dong, *Mont. Not. R. Astron. Soc.* **523**, 928–933 (2023).